MECHANICAL AND TRIBOLOGICAL CHARACTERIZATION OF PARTICULATE FILLED AL7075 ALLOY HYBRID COMPOSITES FOR PISTON RING MATERIAL

A THESIS SUBMITTED IN PARTIAL FULFILLMENT OF THE REQUIREMENTS FOR DEGREE OF

Master of Technology

in

Production Engineering

By

SHIVAM MISHRA

(2013PPE5380)

Under the supervision of

Dr. AMAR PATNAIK

DEPARTMENT OF MECHANICAL ENGINEERING
MALAVIYA NATIONAL INSTITUTE OF TECHNOLOGY JAIPUR-302017
JUNE, 2015

CERTIFICATE

This is to certify that the dissertation entitled **"Mechanical and tribological characterization of particulate filled Al7075 alloy hybrid composites for piston ring material"** being submitted by **SHIVAM MISHRA(2013PPE5380)** is a bonafide work carried out by him under my supervision and guidance, and hence approved for submission to the **Department of Mechanical Engineering, Malaviya National Institute of Technology, Jaipur** in partial fulfillment of the requirements for the award of the degree of **Master of Technology (M.Tech.) in Production Engineering**. The matter embodied in this dissertation report has not been submitted anywhere else for award of any other degree or diploma.

Dr. Amar Patnaik
Assistant Professor
Department of
Mechanical Engineering
MNIT Jaipur
Place: Jaipur
Dated: June 2015

CANDIDATE'S DECLARATION

I hereby declare that the work which is being presented in this dissertation entitled **"Mechanical and tribological characterization of particulate filled Al7075 alloy hybrid composites for piston ring material"** in partial fulfillment of the requirements for the award of the degree of **Master of Technology (M.Tech)** in **Production Engineering**, and submitted to the **Department of Mechanical Engineering, Malaviya National Institute of Technology Jaipur** is an authentic record of my own work carried out by me during a period of one year from July 2014 to June 2015 under the guidance and supervision of **Dr. Amar Pattnaik** of the Department of Mechanical Engineering, Malaviya National Institute of Technology Jaipur.

The matter presented in this dissertation embodies the results of my own work and has not been submitted anywhere else for award of any other degree or diploma.

SHIVAM MISHRA
(2013PPE5380)

This is to certify that the above statement made by the candidate is correct to the best of my knowledge.

Dr. Amar Patnaik
Supervisor

Place: Jaipur
Dated: June 2015

ACKNOWLEDGEMENT

It is indeed a pleasure for me to express my sincere gratitude to those who have always helped me for this dissertation work. With great delight, I acknowledge my indebted thanks to my M.Tech guide **Dr. Amar Patnaik** who has always been a source of inspiration and encouragement for me. His stimulated guidance and unwavering support always motivated me to reach out for, and achieve higher levels of excellence. This dissertation could not have attained its present form, both in content and presentation without his active interest, direction and help. I am grateful to him for keeping trust in me in all circumstances. I thank him for being big-hearted with any amateurish mistakes of mine.

I extend my deep sense of gratitude to **Prof. I. K. Bhat**, Director, MNIT Jaipur for strengthening the research environment of institute by providing all necessary facilities to students.

I express my sincere gratitude to **Prof. G. S. Dangayach (HOD), Mr. Amit Pancharya , Dr. H. S. Mali and Mr. Mukesh kumar** for their support and guidance throughout the course of study at MNIT Jaipur. I am extremely thankful to all members of Advanced Research Center for Tribology for giving me a continuous support throughout my thesis work. I am also thankful to staff of Mechanical Engineering Department, Metallurgy Department and Material Research Center for their valuable support in the laboratory related work.

I sincerely thank **Mr. Tusar** director of Abilities India Pistons & Rings Ltd and **Dr. M. S. Ramaprasad** for their kind support and appreciable involvement in the completion of thesis work.

I am also grateful to my friend's, parents and my family for their tremendous amount of inspiration and moral support. I am highly indebted and thankful to them for bearing me with endurance and providing their fullest possible co-operation. Finally, but most importantly, I thank Almighty God, for giving me the will power and strength to make it this far when I didn't see a light.

SHIVAM MISHRA

ABSTRACT

To meet the present requirements of the automotive industry, continuous search is done to improve the performance, exhaust emission, and life of the IC engines. In engine assembly piston ring is a critical component. It is small in size but plays very important role in proper working of engine. Piston rings for current internal combustion engines have to meet all the requirements of a dynamic seal for linear motion that operates under demanding thermal and chemical conditions. Due to the continuous reciprocation of the ring on the cylinder liner there is wear and friction between these two. This friction and wear results in frictional loses and problem in functionality of piston ring which finally effects the efficiency of engine and also responsible for the undesirable emissions.

The aim of present investigation is to develop a Metal Matrix Composite having all the properties compatible to that of the currently used material i.e. cast iron for the Piston Ring. They are likely to overcome the performance barrier as there are for a monolithic material like cast iron. Here Al7075 is taken as matrix material with two different reinforcement Fly ash/Graphite and Garnet/Graphite. Al7075 is used due to its low density and good mechanical properties and requirement of composite prevailed from literature reviews to overcome the limitations of Aluminium to be used as Piston ring material. Since the elastic modulus, strength, conductivity, coefficient of thermal expansion, impact strength, wear and friction of material are all vital properties for a piston ring, the present investigation aims at studying all these properties in the Al7075 alloy reinforced Fly ash/Graphite and Garnet/Graphite particulate filled hybrid composites. Taguchi analysis is done to find the influence of different factor on wear rate of the composites.

Improved wear resistance, elastic modulus, tensile strength is found for developed composites. The hardness increased from 33HRB to 88 HRB while the tensile strength and elastic modulus increased from 205MPa to 263 MPa and 69 GPa to 139 GPa respectively.

CONTENTS

LIST OF FIGURES

*****

LIST OF TABLES

***

1.1 BACKGROUND AND MOTIVATION

India is in phase of development, the large population and more consumption of resources barred the growth of country. India is the 6th largest consumer of petroleum. Around 70% of the demands are nourished by the imports of oil and natural gas .So in India, fuel economy is very potential issue and It becomes very important to control the fuel consumption by improving the fuel economy of engine [1].

Environmental protection is another important issue. We all are worried about increasing amount of pollution in air due to increase in the number of vehicles. As the number of vehicles is increasing, it becomes essential requirement of the automobile industries to reduce the emissions to control the content of pollutants within the limits. The level of air quality is necessary within an adequate margin of safety, to guard the public health, vegetation and property [2].

In this new era of development in the automobile industry, fuel economy and environmental protection are the major concerns. A lot of efforts are made by number of researchers for the improvements of engine efficiency and to reduce emissions. Frictional loses due to sliding contact of piston ring and cylinder liner accounts for a 20% of total mechanical loses in the engine. One of the ways to aid in an automobile's fuel economy is to remove the cast iron cylinder block liners and piston ring and replace them with a lighter, more thermally efficient Al-alloy composite which reduces vehicle weight and friction loss simultaneously [3-5].

Al-alloy Metal matrix composite provides better conformability which reduces the emissions. The amount of emission increases with the time. The emissions from the old vehicles are more. Wear of piston ring is responsible for this increase in emission. By using the AMC the emissions due to worn piston ring can be controlled [6].

1.2 PISTON RING

1.2.1 Introduction

A piston ring is a riven ring that fits into a groove on the outer diameter of a piston in a reciprocating engine such as an internal combustion engine or steam engine. There are two entirely different points of view that make dynamic seals particularly demanding in a tribological sense .Firstly, dynamic seals support the cleanliness of a lubricant and a tribological element to be protected from external contamination, and thus adds to suppressing wear by three-body abrasion produced by contaminant particles. At the same time the seal suppresses the leakage of lubricant from the tribosystem, which is an issue of increasing significance for environmental protection and hygiene. Secondly, the counter surfaces of a dynamic seal operate under the same tribological laws as any sliding couples, though with the necessities of low friction and low wear and a long service lifecycle. Seals for linear motion are mainly challenging as their counter surface uniformity, direction of sliding, speed and lubrication tend to vary more than in the closed contact forming a seal for a rotating motion.[7]

(a)	(b)
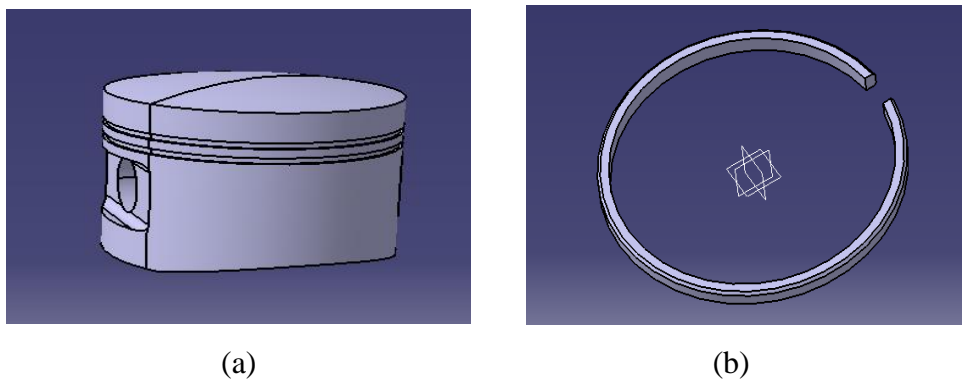
Figure 1.1 CATIA image of (a) Piston (b) Piston ring

Piston rings for current internal combustion engines have to meet all the requirements of a dynamic seal for linear motion that operates under demanding thermal and chemical conditions. In brief, the following requirements for piston rings can be identified:

➢ Low friction, for supporting a high power efficiency rate

➢ Low wear of the ring, for ensuring a long operational lifetime

➢ Low wear of the cylinder liner, for retaining the wanted surface texture of the liner

➢ Emission suppression, by limiting the flow of engine oil to the combustion chamber

➢ Good sealing ability and low blow-by for supporting the power efficiency rate

- ➢ Good resistance against mechano-thermal fatigue, chemical assaults and hot erosion
- ➢ Reliable operation and price effectiveness for a significantly long time.
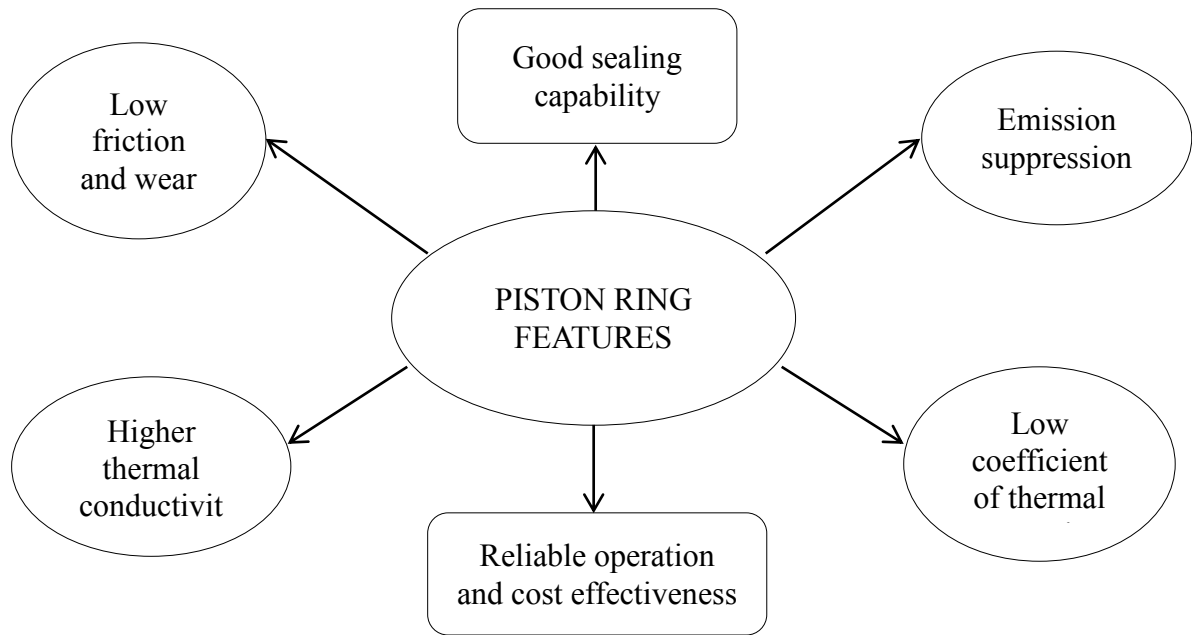
Figure 1.2 Features of Piston Ring

1.2.2 Piston ring mechanics

One of the major requirements on the ring pack is related to the ring dynamics; radial and axial ring motion and ring twist. Ring motion and ring twist about the ring centre affect the operation of the ring, the oil film formation and the friction between the ring and the liner, the wear of the ring and cylinder liner, and the blow-by across the ring pack.
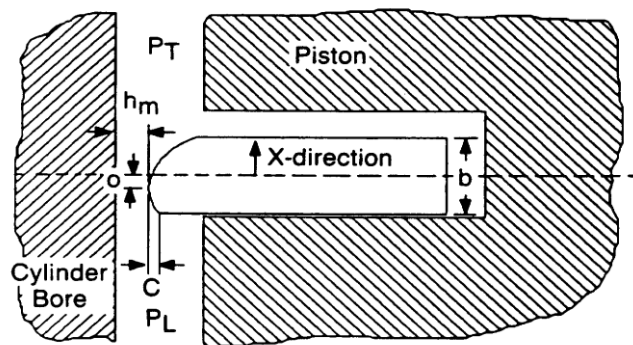
Figure 1.3 Piston Ring, Cylinder and Piston conjunction [2]

The primary motion of the piston rings is equal to the reciprocating piston motion. In an analysis of the piston ring lubrication, it is necessary to determine the velocity of the piston ring as a function of the crank angle. The crank mechanics is shown in Fig. 4. The instantaneous speed of the reciprocating piston motion can be estimated with Maass and Klier[8] formula decent accuracy with the following (, 1981):

$$v_p \approx r\omega \,(\sin\phi + \lambda/2 \sin 2 \phi) \tag{1.1}$$

$$a_p \approx \omega \, 2r(\cos\phi +\lambda \cos 2\phi \tag{1.2}$$

where v_p is instantaneous piston speed, a_p is instantaneous piston acceleration, r is crank radius, ω is angular velocity of the crank, ϕ is crank angle, $\lambda = r/l$, l is con rod length

(a)   (b)
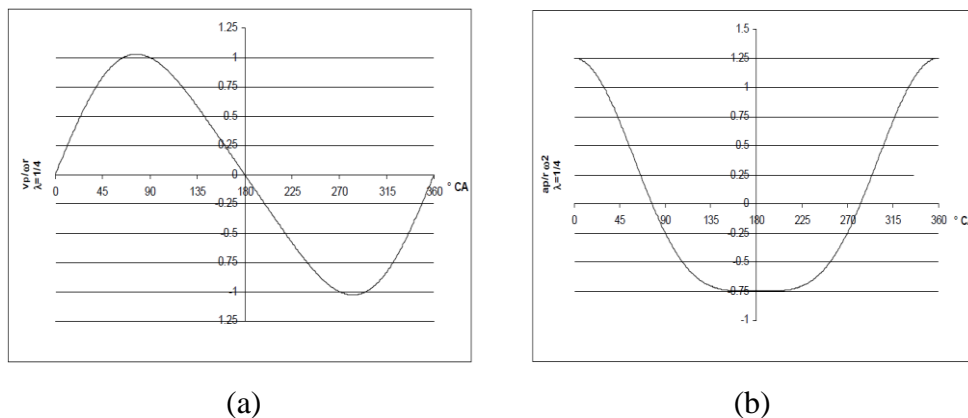
Figure 1.4 (a) Velocity variation of Piston with crank angle (b)Acceleration variation of Piston[11]

With the above primary motion of the piston, the also have a secondary motion which is investigated by number of researchers. This secondary motion of the piston is very much responsible for the unpredictable tribological behavior of piston ring. So it becomes very important to study and understand the secondary motion i.e. the tilting of piston about its axis. Tan et al. described the motion of piston ring from BDC to TDC inside the cylinder. Fig. 4 shows the piston orientation at different position in its motion path. Fig 5 shows graphical representation of stroke length and tilt angle with stroke position [3].
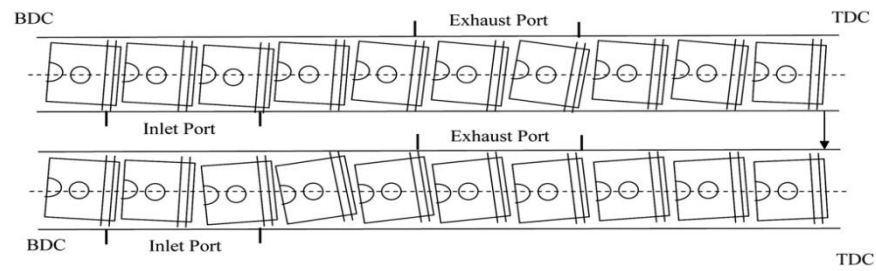
(a)
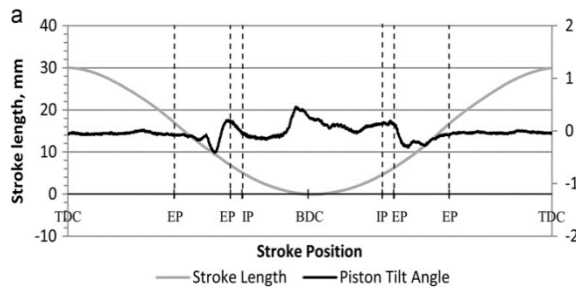
(b)
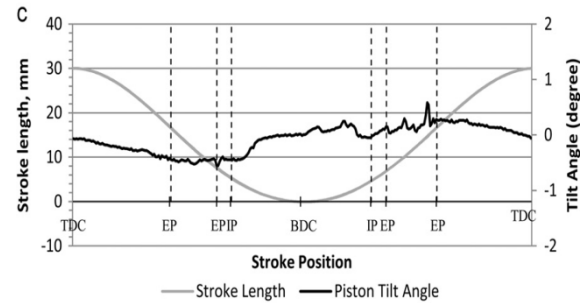
(c)

Figure 1.5 (a) Secondary motion of piston ring from TDC to BDC, Graphical representation of variation in stroke length and tilt angle (b) 100 rpm (c) 600 rpm[3]

1.2.3 Piston ring forces and moments

The piston ring secondary motions can be divided into piston ring motion in the transverse direction, piston ring rotation, ring lift, and ring twist. These types of motion result from different loads acting on the rings. Loads of this type are inertia loads arising from the piston acceleration and deceleration, oil film damping loads, loads due to the pressure difference across the ring, and friction loads from the sliding contact between the ring and cylinder liner. The forces acting on the ring are presented in Fig. 5.7 [9].

The gas pressure above, below and behind the ring develops resultant forces on the ring segment. The inertia forces acting on the piston rings, in addition to those acting on the other reciprocating crank mechanism components, change proportionally to the square of the engine speed. The side loading of the piston against the cylinder wall is a result of the articulated joint of the connecting rod. The effect of the clearance between the cylinder liner and the piston on the piston and piston ring motion and to the ring forces is presented in Fig. 1.3. The shearing of the lubricating film, the sliding friction forces and the contact pressure between the ring and the liner cause normal and tangential forces on the ring face. The elastic distortion of the piston and liner can

affect the effective geometry of the ring face and cylinder liner contact, which causes a non-uniform distribution of the contact pressure between the cylinder liner and the piston ring face and can thus lead to increased blow-by and oil consumption.[10]

(a)   (b)
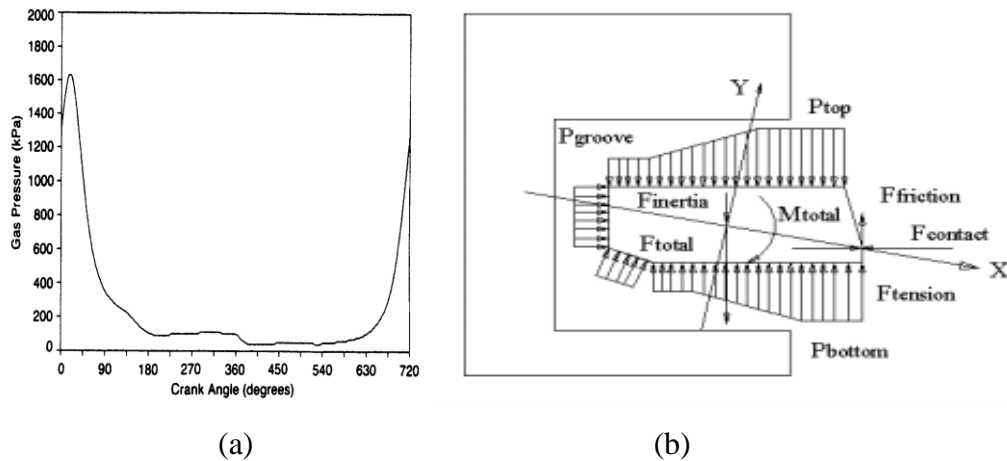
Figure 1.6 (a) Variation of gas pressure with respect to crank angle[2](b) Force distribution on Piston ring[11]

The piston pin is often offset from the piston centre line. This arrangement is applied in order to avoid piston-generated noise or to reduce the thermal load on the ring grooves [11]. Haddad and Tjan[13] have used a computer program to observe the influence of the offset of a piston pin, centre of gravity, and crank offset from the bore centre line, on the mechanical performance and engine noise. The results presented conclude that, generally, the kinetic energy loss decreases when the piston pin offset is set to the thrust side of the piston and the mechanical efficiency increases when the piston pin offset is set to the minor thrust side of the piston. In the conclusions of their work, the authors specified that the piston pin offset is the most sensitive parameter producing considerable variations in kinetic energy loss and mechanical efficiency. Additionally, the kinetic energy loss can be reduced, and the mechanical efficiency can be increased by setting the piston pin offset to the thrust side of the piston centre. H. Chittenden and Priest [14] have observed the same kind of results. According to their predictions, the contact situation will be worse and the friction losses will increase if the piston pin offset is positioned towards the minor thrust side of the piston.

1.3 COMPOSITE MATERIALS

1.3.1 Introduction

Composite material is a material composed of two or more distinct phases (matrix phase and reinforcing phase) and having bulk properties significantly different from those of any of the constituents. Many of common materials (metals, alloys, doped ceramics and polymers mixed with additives) also have a small amount of dispersed phases in their structures, though they are not considered as composite materials since their properties are similar to those of their base constituents (physical property of steel are similar to those of pure iron) . Promising properties of composites materials are low density, high stiffness, high strength, high temperature stability, high electrical and thermal conductivity, modifiable coefficient of thermal expansion, corrosion resistance, better wear resistance etc.

Among the advanced engineering materials for aerospace and automotive applications, Al-based metal matrix composite (MMCs) are of great interest due to their appreciable mechanical properties, with low density, high elastic modulus and strength, and good fatigue and wear resistance [1–5]. The driving force behind the development of MMCs is the possibility to tailor their properties to meet desired requirements, which render such types of materials unique in comparison with conventional unreinforced materials. Composites consist to different phases which are-

Matrix phase

The primary phase, matrix is defined as the monolithic material which binds the reinforced material without any chemical bonding between them. Generally matrix materials used are ductile and light in weight.

Reinforcing phase

Second phase (or phases), reinforcement is a more strong and hard part of composite which are embedded in the matrix in different can be fiber, whisker or particle form.

Composites as engineering materials usually refer to the material with the following characteristics:

1. These are artificially made (excluding natural material such as wood).

2. These consist of at least two different species with a well defined interface.

3. Their properties are influenced by the volume percentage of ingredients.

4. These have at least one property not possessed by the individual constituents.

Performance of Composite depends on:

1. Properties of matrix and reinforcement,

2. Size and dispersal of constituents

3. Shape of constituents

4. Nature of interface between constituents.

1.3.2 Classification of composites
Composite materials are classified

A. On the basis of matrix material,

B. On the basis of filler material.

1.3.2.1 On the basis of Matrix:

1. Metal Matrix Composites (MMC)

Metal Matrix Composites are composed of a metal matrix (Aluminum, Magnesium, Iron, Cobalt, Copper) and a dispersed ceramic (oxides, carbides) or metallic (lead, tungsten, molybdenum) phase.

2. Ceramic Matrix Composites (CMC)

Ceramic Matrix Composites are composed of a ceramic matrix and embedded fibers of other ceramic material (dispersed phase).

3. Polymer Matrix Composites (PMC)

Polymer Matrix Composites are composed of a matrix from thermoset (Unsaturated polyester (UP), Epoxy) or thermoplastic (PVC, Nylon, Polystyrene) and embedded glass, carbon, steel or Kevlar fibers (dispersed phase).

1.3.2.2 On the basis of type of Reinforcement:

(a) Particle reinforced Metal matrix composites

These composites generally contain equiaxed ceramic reinforcements. Ceramic reinforcements are generally oxides or carbides or borides (Al_2O_3 or SiC or TiB_2) and present in volume fraction less than 30% when used for structural and wear resistance applications. In general, PAMCs are manufactured either by solid state (PM processing) or liquid state (stir casting, infiltration and in-situ) processes. PAMCs are less expensive compared to CFAMCs. Mechanical properties of PAMCs are inferior compared to whisker/short fiber/continuous fiber reinforced AMCs but far superior compared to unreinforced Aluminium alloys. These composites are isotropic in nature

and can be subjected to a variety of secondary forming operations including extrusion, rolling and forging.

(b) Short fiber- and whisker-reinforced Metal matrix composites

These contain reinforcements which are not continuous. Short alumina fiber reinforced Aluminium matrix composites is one of the first and most popular AMCs to be developed and used in pistons. These were produced by squeeze infiltration process. Whisker reinforced composites are produced by either by PM processing or by infiltration route. Mechanical properties of whisker reinforced composites are superior compared to particle or short fiber reinforced composites. Though, in the recent years usage of whiskers as reinforcements in AMCs is fading due to perceived health hazards and, hence of late commercial exploitation of whisker reinforced composites has been very limited. Short fiber reinforced AMCs display characteristics in between that of continuous fiber and particle reinforced AMCs.

(c) Continuous fiber-reinforced Metal matrix composites

Here, the reinforcements are in the form of continuous fibers (of alumina, SiC or carbon). The fibers can either be parallel or pre interlaced, plaited prior to the production of the composite. AMCs with fiber volume fraction up to 40% are produced by squeeze infiltration technique.

The main focus of the research is development of particulate/ fiber filled metal matrix alloy composites by stir casting technique and study of their physical, mechanical, and thermal characterization. Finally, study of stress intensity factor (single edge) of the fabricated composites in experimentally and validated with the finite element simulated results and exist theoretical models.

1.4 OBJECTIVE OF THE PRESENT WORK
1. Study of Piston ring material design and manufacturing.
2. Study of tribology involved in Piston Ring.
3. Study Physical, Mechanical, Thermal and Wear characterization of particulate filled Al alloy composites.
4. Develop series of composites for Physical, Mechanical and Thermal characterization.
5. Reciprocating friction and wear analysis of developed composite.
6. Implementation of design of experiment (DOE) and optimization technique.
7. FEM analysis of composite and piston ring.

Thesis outline

This manuscript is organized into following chapters (brief description of the chapter).

Chapter 2: Includes a literature review designed to provide a summary of the base of knowledge already available involving the issues of interest. This chapter presents the research works on aluminium matrix composites by various investigators.

Chapter 3: This chapter briefly explains the selected method and materials for the research work, different combination of compositions, fabrication methodology, various theoretical method of calculation of properties (density ,void-fraction, tensile strength, elastic modulus, wear) with experimental and by FEM-modeling method.

Chapter 4: This chapter includes theoretical, experimental and FEM modeling based mechanical analysis of fabricated composites.

Chapter 5: This chapter includes the effect of particulate (Garnet/Graphite and Flyash/Graphite) content on reciprocating wear behavior of A7075 alloy composites. Optimization of different parameter with the help of Taguchi method is also presented in this chapter.

Chapter 6: This chapter includes the FEM analysis of composite Piston Ring with the help of ANSYS software.

Chapter 7: This chapter includes a comparative analysis of conventional piston ring materials (Cast Iron and steel) and fabricated composites

Chapter 8: Provides summary, specific conclusions drawn from both the experimental and analytical efforts and recommendations for future research.

*****

2.1 INTRODUCTION

The purpose of this literature review is to enlighten past research work done in the areas related to the present study. The various aspects of the metal matrix composites as found in the literature in relation to the under mentioned topics are exhaustively reviewed. The topics included in the literature review are:

➢ Study of Piston Ring material.

➢ Effect of filler content on physical and mechanical properties of metal matrix composites (MMCs).

➢ Effect of filler content on tribological characteristics of MMCs.

➢ Finite element analysis of MMCs.

➢ Implementation of design of experiment (DOE) and optimization technique

At the end of this chapter, the research gaps and the objectives deduced from the literature review are presented.

2.2 STUDY OF PISTON RING MATERIAL

In the starting phase there was no piston in the steam engines. Then first ring was introduced by Ramsbottom in 1854 the hole work of this ring was to compress the gas. After this a continuous effort was given by the researchers in improvement of design and the material for improving the functionality of the piston ring. Miller, in 1862 introduced a modified design of Ramsbottom ring which facilitated the design to use the gas pressure from the back side of the ring to provide better sealing force.[7] Grey cast iron is one of the most used materials for the piston ring application because of its unique properties like self-lubrication due to presence of graphite flacks and oil retaining capacity which provides oil in oil starvation condition. Number of coatings is available for the piston ring to improve the functionality of piston rings. Chromium coating on ring is done to protect it from sever abrasive and corrosive environment. Molybdenum coating provide self-lubrication in the dry condition and also improve the conductivity.

Dufrane and Radil [15] in their experimental work of coating of ring with molybdenum-nickel-chromium alloys, chromium oxide (Cr_2O_3) with metallic chromium binder by thermal spraying method observed that Hard chromium layers can be improved by plasma spraying chromium ceramic on the ring face, therefore increasing the thermal load capacity. Haselkorn and Kelley [16] have investigated coatings for use in low-heat rejection engines. They conclude that high carbon iron-molybdenum blend and chrome-silica composite applied by plasma spray, and further chrome nitride applied by low-temperature arc vapour are coatings with properties that meet the demands in low-heat rejection engines. Dowson et al.[11] in his experimental work in actual environment of piston ring assembly observed that the gas pressure above, below and behind the ring produces resultant forces on the ring section, The inertia forces acting on the piston rings, as well as those acting on the other reciprocating crank mechanism components, change proportionally to the square of the engine speed.

Engines have changed greatly during the last 25 years. New, high-powered engines require rigid maintenance procedures, much more so than older engines. Basic procedures for overhauls remain about the same, but each portion of maintaining and rebuilding is more critical. In spite of continuous evolution and research on pistons, its failure is still a common phenomenon. It is the only component of the engine that encounters failure from different origins: thermo-mechanical stresses, wear, fatigue, extreme temperatures, oxidations, etc. and engine operating conditions like lean carburetor jetting, advanced ignition timing, foreign material trapped inside, inappropriate piston-to-cylinder clearance, low octane fuel, loss of lubrication, high compression ratio, etc. With increasing demands for quieter, cleaner, faster and powerful engines, failure of engines and its subsystems like piston rings has also increased proportionately. Many significant developments have been achieved in abridging and understanding the mechanisms of failures. Notwithstanding with the advanced developments, there still exists significant challenges that needs to be addressed [7].

Engine oils with and without friction-reducing additives have been investigated by Glidewell et al[17] who conclude that friction in fully flooded conditions with MoDTC is clearly lower than with non-friction-modified oils. He observed the wear rate with different friction modifiers (ex:-ZDDP, Molybdenum dialkyl-thiocarbamate

(MoDTC)).In starvation conditions the friction with the MoDTC-modified oil may decrease to become equal to that of non-friction modified oils. With age, the friction-reducing effect of MoDTC seems to degrade. Glaeser et al.[18] observed that under conditions of lubricating oil starvation, grey cast iron provides certain reduction in the friction forces, by the lubrication effect of the graphite phase and by the oil reservoir provided by the graphite phase of the material.

Dearlove and Cheng[19] have measured the coefficient of friction of a chromium plated piston ring with a barrel profile oscillating against a polished and honed cast iron cylinder liner sample under lubrication with five different oils at 30°C temperature, and they report average coefficient of friction of approximately $\mu = 0.07$ at mid-down stroke, at 200 rpm engine speed and 40...80 N normal force. At an engine speed of 400 rpm, the corresponding coefficient of friction was approximately $\mu = 0.06$, and at 600 rpm the value was $\mu = 0.03$.

Experiments by Takiguchi et al.[20] with two ring and three-ring pistons have shown that the number of rings influences the frictional behavior of the ring pack, but that the total tension of the piston rings in the ring pack finally determines the friction losses. Truhan et al.[4] have done improved laboratory test to evaluate the friction and wear behavior of ring and liner material by using more realistic lubricants.(Jet aviation fuel,Reagent grade mineral oil,heavy duty SAE 15W40 oil,aged SAE 15W40).Cameran plint high frequency test rig was used for testing and Cromium coated ductile iron was used as specimen. The experimental results of ring and cast iron flat was plotted and compared with the results of derived from geometric model. The minimum and maximum wears are found aged SAE 15W40 and Jet aviation fuel respectively.

Singh et al.[5] investigated problem of seizure failure of piston experimentally with numerical simulation. He reported that this was due to the direct contact of piston and cylinder liner and it was due to wear out of piston ring. Mittle et al.[21] studied the emissions characteristics in IC engine and found different type of pollutants in exhaust gases and found that one of the reasons for increase in emission is wear of piston ring.

2.3 EFFECT OF FILLER CONTENT ON PHYSICAL AND MECHANICAL PROPERTIES OF MMCS

Among the advanced engineering materials for aerospace and automotive applications, Al-based metal matrix composite (MMCs) are of great interest due to their appreciable mechanical properties, including low density, high elastic modulus and strength, and good fatigue strength . The driving force behind the development of MMCs is the possibility to tailor their properties to meet desired requirements, which render such types of materials unique in comparison with conventional unreinforced materials.

Kamat et al.[22] studied the mechanical properties of Al2024 alloy composite reinforced with alumina and observed that yield and ultimate tensile strength of the composite increased with increase in volume fraction of Al2O3 particles. Breval[23] in his review on synthesis routes to metal matrix composites with specific properties found that the hardness, modulus of elasticity and electrical resistivity do not change significantly below 25 wt.-% of reinforcement, whereas the fracture toughness increases significantly, even with small metal additions.

Yoshihiro et al.[24] studied the deformation behavior of PFMMC and found that the main cause of the increase of the deformation resistance in the plastic range is the gradient appearing in the matrix material, which increases with the reduction of the distance between particles.

Fabrication of MMCs has several challenges like porosity formation, poor wettability and improper distribution of reinforcement. Achieving uniform distribution of reinforcement is the foremost important work. A new technique of fabricating cast Aluminium matrix composite was used for uniform distribution of particles within the matrix by number of researchers i.e. double stir casting method [25-30]

Mechanical properties of the ceramic filled MMCs are investigated by number of researchers and improved Tensile strength, Elastic modulus and wear resistance informed[36-39]. Azim et al.[40] developed Al2024/ Al2O3p composite and investigated its mechanical properties. They observed that yield strength of the composite increased while ultimate tensile strength and ductility decreased with increase in volume percentage of ceramic filler. Ceramic materials offers great potential for development as a high strength and high temperature refractory

materials, so it is amongst the most preferred materials used as the reinforcement for the fabrication of particulate filled metal matrix composites.

Llorca and Gonzalez [41] studied the microstructural factors controlling the strength and ductility of particle reinforced metal matrix composites and found that microstructural factors can be combined to provide an optimum combination of strength and ductility. Tee et al. [42] developed in situ Al-TiB2 composite by stir casting. The authors observed that the tensile and the yield strength of the composite was twice that that of unreinforced matrix but the ductility showed a lower value. Tjong and Ma [43] reviewed the microstructural and mechanical characteristics of in situ metal matrix composites (in which the reinforcements are formed in situ by exothermal reactions between elements or between elements and compounds) and found that the MMCs so produced exhibit excellent mechanical properties. Veeresh Kumar et al.[44] reported that the micro-hardness (HV) of Al6063-SiC and Al7075-Al2O3 composites increased with the percentage of filler addition and that of Al7075-Al2O3 composites was observed more as compared to that of Al6063-SiC composites. Lakshmipathy et al.[8] comparatively studied the behavior of Al7075/SiC and Al6061/Al2O3 and observed that hardness was increasing while impact strength was deceasing with increase in filler content and they also observed the better results for Al7075 matrix MMCs.

The metal matrix composites are often used in some harsh environments and working processes, for example, high temperature and high pressure, as well as thermal shock and so on. In the thermal shock environment, it is important to predict thermo-mechanical behavior and interfacial stress of metal matrix composites. Ju D.Y.[45] used thermo-mechanical theory to simulate the thermal shock process of metal matrix composite and found that the temperature and stresses based on the coupled analysis can present jump behavior of stress on the interface of the MMCs.

Ruggles [46] studied the uniaxial and biaxial rate-dependent behavior of a discontinuous metal-matrix composite at 538 °C and found that the titanium alloy (Ti-6Al-4V) reinforced with TiC particles (10% by weight) can be idealized as an isotropic, pseudo homogeneous continuum, and may be modeled with the unified viscoplasticity theories developed for engineering alloys.

Spiridonova and Sukhova [47] studied metal matrix composites containing Cr-20Ti-10C reinforcement fabricated by infiltrating at 1200 °C to 1280 °C for 30 to 60 min

and concluded that the copper weakly wets Cr-20Ti-10C that does not form any new phases when reacting with liquid copper. The wettability can be improved by adding 20 % Mn to copper. Similar study on the infiltration of ceramic particle was carried by Taha and Nahed [48] based on the particle distribution and the metal ceramic interface.

Cordovilla et al. [49] concluded that the increase in the hardness of the composites, containing hard ceramic particles not only depends on the size of reinforcement but also on the structure of the composite and good interface bonding. Alaneme et al.[50] investigated the mechanical and corrosion behaviour of SiC bamboo ash reinforced Al-Mg-Si alloy hybrid composite. The author reported that the ultimate tensile strength, hardness and yield strength values of the composite decreased with increase in percentage weight of bamboo leaf ash while the fracture toughness of the hybrid composite was superior. Corrosion resistance of the hybrid composite was superior in basic solution as compared to acidic solution.

Kouzeli et al. [51] studied the tensile behavior of pure aluminium reinforced with $\geq$ 40 vol.-% alumina particles and found that the initial stiffness of infiltrated Al_2O_3–Al composites is controlled by the volume fraction of reinforcement, while the yield stress is a function primarily of particle size. Neither of these properties is significantly influenced by the shape of the reinforcement. Li et al. [52] experimentally found that the maximum liquid phase sintering temperature for Al 4.5%Cu/15%SiC metal matrix composite can be increased to about 1.63% in comparison with its matrix material and by some simplifications in the model, the relationship between the amounts of liquid phase, particulate size, cluster size and degree of distribution of reinforcements can be understood. The analytical model suggested by Li et al. [52] based on the particle size and cluster effects on particulate-filled composite concluded that with hard particles, the stress and strain concentrations occur in the matrix, which is at the interface of the particle and the matrix, in radial direction. Reinforcing bonding strength at the interface and enhancing the deformability of the matrix are required. Azim et al.[53] investigated the mechanical and wear properties of the stir cast AlSi18CuNi/ Al2O3p composite. Authors observed that the tensile strength and hardness of Al2O3 filled matrix was much improved and the wear resistance is also improved.

The reinforcement weight fraction plays an important role in affecting the mechanical properties and behaviour of the composite. The composite shows different properties

at different weight percentage of reinforcement. The percentage of the reinforcement to be added in the matrix material depends on the application of the composite. Tzamtzis et al. [54] adopted Rheo-process to produce A356/SiCp composites and found an improved distribution of reinforcement in the matrix with improved ultimate tensile strength and tensile elongation. Xu and Zong [55] selected SiC and Al_2O_3 (10-20 vol.-%) particle reinforced Al-2618 matrix composites subjected to tensile loading to simulate stress-strain curve and average stress in particles and predicted that the stress in reinforcing particle during straining is found much higher than that in matrix. In another study, Zong et al. [56] found that micro-mechanical models play only minus role in strengthening the particulate reinforced aluminium matrix composites with a precipitated hard matrix.

Chou et al. [57] fabricated Al_2O_3/A356, Al_2O_3/6061 and Al_2O_3/1050 composites, respectively; with different volumes of aluminum alloy content by squeeze casting and concluded that relative density of the composites were the most important factors to affect the mechanical properties and the three different toughening mechanisms, i.e. crack bridging, crack deflection and crack branching in the composites. Kok [58] fabricated Al2024/ Al2O3p composite and studied its mechanical properties. The author has revealed that the hardness and tensile strength of the composite with increasing the weight percentage of the reinforcement. Amirkhanlou et al.[59] evaluated the hardness and impact energy of the Al(A356)/SiCp composite and observed that the hardness and the impact energy of the composite was higher compared to the pure alloy. Alaneme et al.[59] reported that ultimate tensile strength, yield strength, specific strength and percent elongation of rise husk and alumina reinforced Al-Mg-Si alloy hybrid composites decreased with the increase in filler content, and this trend was due to the presence of rice husk, which has lower hardness and strength values in comparison with SiC.

Kakaiselvan et al.[62] fabricated Al6061/B4C MMCs and investigated its mechanical properties. They found that the hardness and the tensile strength of the composite are linearly increasing with increasing weight percentage of the B4C particulate. Boopathi et al.[60] in their study found that the presence of SiC and fly ash in Al2024 alloy improved its tensile strength and yield strength, however reduced its ductility. Mazaheri et al.[47] performed a comparative study of mechanical properties of Al/TiC, Al/B4C and Al/TiC/B4C hybrid composite. The author has revealed that

Al/TiC/B4C composite possessed highest hardness. Highest yield strength and tensile strength was shown by Al/B4C composite and Al/TiC showed maximum elongation. Jayaram and Biswas [61] investigated rupture strengths of SiC reinforced Si-Zn-Mg-based Al matrix composite samples by the three-point bend test, which did not show any trend with the increase in particulate size, and it was found to be maximum (200 MPa) for the composites with SiC particle size of 25 and 67 μm. Kumar et al.[62] developed A359/ Al2O3 composite via electromagnetic stir casting method. The author revealed that the hardness values increased to 72.8 HRC compared to pure alloy (46HRC). Also the tensile strength of the composite increased to 148.7N/mm2 as compared to pure alloy (103.7N/mm2).

2.4 EFFECT OF FILLER ON TRIBOLOGICAL CHARACTERISTICS OF MMCS

Aluminium-based metal matrix composites are well known for their high specific strength, stiffness and hardness. They are gaining further importance as their potential for wear resistance has been established. In general, for sliding against metals and abrasives, many studies have reported that composites exhibit better wear resistance than the unreinforced alloys [61-66]. Designers are changing over to ceramic materials and ceramic reinforced materials for improvement in wear resistance, corrosion resistance and high thermal strength [67-68].

Lakshmipathy et al. [8] comparatively studied the wear behavior of Al7075/SiC and Al6061/Al_2O_3 and observed that wear resistance was increasing with increase in filler content and they also observed the better results for Al7075 matrix MMCs. Sharma et al.[82] evaluated the wear behavior of Al(LM13) reinforced with garnet. And it was found that the wear resistance increase with garnet content but decrease with the size. Wear performances of particulate reinforced aluminium matrix composites reinforced with Garnet were investigated by S.C. Sharma[29] and found that the wear resistance of Al6061 matrix, garnet particulate reinforced composites are superior to that of unreinforced matrix alloy, their wear resistance increases with increasing wt.% of garnet and it was due to the formation of mechanical mixed layer(MML).

The tribological parameters that control the friction and wear performance of MMCs like load, sliding velocity, sliding distance, reinforcement size and reinforcement volume fraction have been reviewed in detail by Sannino and Rack[65]. Narayan et al. [66] investigated Al2024 15 vol.-% Al_2O_3 particulate filled composite and concluded

that it shows better seizure resistance than does the unreinforced alloy in the peak-aged condition.

Pruthviraj [67] reported wear characteristics of Chilled Zinc-Aluminium Alloy reinforced with silicon carbide particulate composites and found that wear resistance of Zn-Al can be improved remarkably by the incorporation of hard particles to form MMCs. Wang et al. [68] fabricated novel aluminium alloy matrix composites reinforced by 15 vol.-% Ni_3Al intermetallic particles and discussed the relationship between wear rate, surface structural changes and starting microstructure. Ye H [69] studied the development of Al-Si alloy and its based material for engine application and found that higher silicon content usually increases the wear resistance of Al-Si alloy as it increases the alloy's hardness. A similar study based on the aluminum metal–matrix composites for automotive applications was carried out by Prasada and Asthana [70] and determined that reinforcement of aluminum alloys with solid lubricants, hard ceramic particles, short fibers and whiskers results in advanced metal–matrix composites (MMC) with precise balances of mechanical, physical and tribological characteristics. Arik et al. [71] performed an experiment on wear tests using a pin on-disc wear tester under dry sliding condition and concluded that the formation of stable iron based mechanical mixed layer on the surface of $Al–Al_4C_3$ composite during the dry sliding at low applied loads resulted in low wear of MMCs. In a similar test performed by Kennedy et al. [72], it was concluded that CuSiCp MMC materials wore less than cast iron on both friction material counter faces. Lim et al. [73] studied the tribological properties of Al-Cu/SiCp metal-matrix composites fabricated using the rheocasting technique and found that the rheocast samples exhibited a better wear resistance at higher loads when compared to MMCs having the same composition but fabricated using the powder metallurgy route incorporating mechanical alloying. Dogan et al. [74] studied the wear of titanium carbide reinforced metal matrix composites under different wear condition and concluded that in a low-stress, removal of matrix material between the TiC particles by the abrasive appears to be the primary mechanism of material removal whereas in a high-stress, the larger TiC particles provide better protection for the softer matrices at low to intermediate hardnesses. Gurcan and Baker [75] studied the wear behaviour of AA6061 aluminium alloy and its composites using Saffil , SiCp and mixture of the two and found that containing only Saffil had inferior wear resistance to those containing the same

volume fraction of SiC. It was also found that a small increase in the wear resistance over 20% SiC, AA6061 composites was found for a 11% Saffil + 20% SiC, hybrid composite when tested against SiC grit.

The tribological properties of A357/SiC, A339/SiC, AA6061/SiC and AA6061/Al_2O_3 materials were determined for different ceramic particle sizes and volume fractions by Cordovilla et al. [76]. The results indicated that the specific wear rate of the aluminium alloy/ceramic particulate composites investigated in this work decreases with increasing volume fraction of the reinforcing particulates. The specific wear rate decreases with increasing particle size. Aluminium alloy composites reinforced with SiC particulates are more effective against abrasive wear than those reinforced with Al_2O_3 particulates. The erosion due to the impact of solid particles can either be constructive (material removal desirable) or destructive (material removal undesirable), and therefore, it can be desirable to either minimize or maximize erosion, depending on the application. Zarghani et al. [77] found a significant improvement in wear resistance of Al/Al_2O_3 nano-composite surface layer on an Al alloy substrate in comparison to the as-received substrate. In a recent study, Shivamurthya and Surappa [78] studied the dry sliding wear and friction behaviour of A356 Al alloy and its composites containing 10 and 20 vol.-% SiC_P. SEM and EDAX analysis of worn surfaces of composite discs showed formation of tribolayers, consisting of mixture of oxides of Al, Si, Cu, Ca, Ba, Mg, and Fe. In these layers, copper and barium content found to be increase with sliding speed in the case of composites.

2.5 FINITE ELEMENT ANALYSIS OF MMCS

A typical design process involves iterative analysis which is computationally intensive and time consuming. The finite element method is now a days the most widely accepted computational tool in engineering analysis. Through solid modeling, the component is described to the computer and this description affords sufficient geometric data for the construction of a mesh for finite element modeling. It is easy for a designer to change the parameters of the desired component and to obtain the results using the finite element methods [79-81]. Singh et al.[82] developed an ANSYS based model of the piton and simulated it for the varying temperature and load condition. The authors observed the stress distribution on the piston ring and found the condition of maximum performance for the engine. Segurado and Llorca

[83] developed a new three-dimensional quadratic interface finite element and checked it potential by simulations including sphere fracture in composites made up of random distribution of elastic spheres within an elasto-plastic matrix. Prabu et al. [84] reported that a finite element study of effect of volume fraction of SiC and diameter of the fiber on interfacial stress/strain characteristics of 6061 Al/SiC metal matrix composites and found that the fiber diameter plays an important role in the debonding and the results show that debonding is more pronounced in the interfacial element near the axis of symmetry. The debonding initiated purely by the shear and maximum shear stress occurs just inside the model at some distance from the free end of the unit cell and it propagate as the load increases. Ganguly and Poole [85] simulated the compressive deformation of composite using anisotropic, plane strain finite element model and found that mean values of the experimental measurements of reinforcement hydrostatic stress matched well with the numerical estimates. Prabu and Karunamoorthy [86] reported microstructure-based finite element analysis of particlereinforced metal matrix composite (PRMMC) to evaluate the stress–strain and failure behavior and found from the results that the random particle microstructure undergoes less percentage of particle fracture than particle rich clustering microstructure. In the case of random particle clustering, fewer tendencies for particle fracture were observed.

2.6 IMPLEMENTATION OF DESIGN OF EXPERIMENT (DOE) AND OPTIMIZATION TECHNIQUE:

Wear processes in composites are complex phenomena involving a number of operating variables and it is essential to understand how the wear characteristics of the composites are affected by different operating parameters. Selecting the correct operating conditions is always a major concern as traditional experiment design would require many experimental runs to achieve satisfactory result. In any process, the desired testing parameters are either determined based on experience or by use of a handbook. It, however, does not provide optimal testing parameters for a particular situation. Thus, several mathematical models based on statistical regression techniques have been constructed to select the proper testing conditions [87-89]. Taguchi and Konishi [90] advocated the use of orthogonal arrays and Taguchi [91] devised a new experiment design that applied signal-to-noise ratio with orthogonal arrays to the robust design of products and processes. In this procedure, the effect of a factor is measured by average results and therefore, the experimental results can be

reproducible. Phadke [92], Wu and Moore [93] and others [94-97] have subsequently applied the Taguchi method to design the products and process parameters.

Ravindra et al.[106] investigated the tribological behavior of the Aa 5083/10 Wt. % Sic particles on pin on disc set-up and applied taguchi method for optimization of parameters. Authors observed that the applied load have maximum influence on the wear rate on the alloy. Shiddharta et al.[98] investigated the wear behavior of epoxy–TiO2 particulate filled functionally graded composites materials and found that load play most important role among the all the factors. Patnaik et al[100] studied particulate filled fiber reinforced polymer composite. The experiments were conducted using using Taguchi L27 orthogonal array and the relation between thermal conductivity and wear was established using ANOVA and Genetic Algorithm technique. Erosion wear behavior of material includes effect of number of factors such as impingement angle, erodent velocity, erodent size, composition of material etc. The experiment was conducted using Taguchi L27 Orthogonal array of experiment design and significance of each factor was determined by using techniques like ANOVA, Genetic Algorithm, Artificial Nural Network etc. The percentage contribution of each factor was determined. Ramesh [97] focused on identifying the factors such as filler type, filler loading, filler size, normal applied load and sliding distance on two-body abrasive wear behaviour of the hybrid composites. Abrasive wear tests were carried on carbon fabric reinforced epoxy composite (C-E) filled with filler alumina (Al2O3) and molybdenum disulphide (MoS2) separately in different proportions, using pin-on-disc apparatus. The experiments were planned according to Taguchi L18 orthogonal array by considering five factors, one at two levels and the remaining at three levels, Analysis of variance (ANOVA) was employed to determine the significance of factors influencing wear. Orthogonal array and grey relational analysis was employed to optimize the multi-response characteristics of two-body abrasive wear behaviour of hybrid C-E composites[100-103].

2.6 RESEARCH GAP
From the above literature, the following research gap have been identified for the research work

1. Though lots of research has been done on design of piston ring but very few researches have been done on material, specifically piston ring of composite material.

2. Number of research has been done on ceramic filled al alloy composite but no one has fabricated Al7075/Garner/Graphite and Al7075/Flyash/Graphite hybride composites.

3. Few researchers have used the FEM software ANSYS techniques to analysis on the mechanical properties and fracture toughness behaviour of particulate filled metal alloy composites and Piston Ring.

4. Tribological characteristic of Al7075 aluminium alloy is not advocated by reaserchers to large extent.

5. It very important to study the behavior of piston ring with variation in temperature but very less research has been done with temperature variation condition.

Chapter Summery

This chapter provides an exhaustive literature review on particulate filled metal matrix composite as reported by various researchers. With the help of this literature review the actual problem in the piston rings revealed and the appropriate solutions are recognized.

The next chapter discusses the materials and methods used for the fabrication of composites in this research work.

*****

3.1 INTRODUCTION

This chapter describes the properties of the matrix and the reinforcements selected for the research work. The methods adopted for the fabrication of the composites and then methods used for the testing of the compositesare discussed. This chapter explains the methodology used both in theoretical and FEM analysis for physical and mechanical properties (density, tensile, flexural, impact, hardness, void-fraction, and fracture toughness) of the unfilled and filled alloy composites respectively. At the end, the experimental detail of the reciprocating wear testing has been discussed.

3.2 MATRIX MATERIAL

A particulate filled metal matrix composite consists of a metal or metal alloy as matrix material. And in the present study Al7075 alloy is used as the matrix material. Al7075 is one of the highest strength alloy among alloys of aluminium. Additionally, it has some other unique combination of properties like lowdensity, good machinability, good castability, corrosion resistance and wear resistance which makes this more compatible to be used as matrix material for the composite for piston ring. Al7075 rod(fig) used for the fabrication of the composite.

Figure 3.1 Al7075 in rode form (small pieces)

Al7075 Aluminum alloy is used as the matrix material in the present investigation and has the chemical composition as shown in Table 1. The aluminium alloy was reinforced with 2% Graphite and 3% to 9% Garnet to develop the composite through double stir casting method. X-ray diffraction test shows

Table 1

Composition of Al7075 Alloy [8]								
Material	Fe	Cu	Mn	Mg	Zn	Ti	Cr	Si	Al
Percentage	0.21	1.5	0.07	2.4	5.7	0.05	0.19	0.11	Remainder
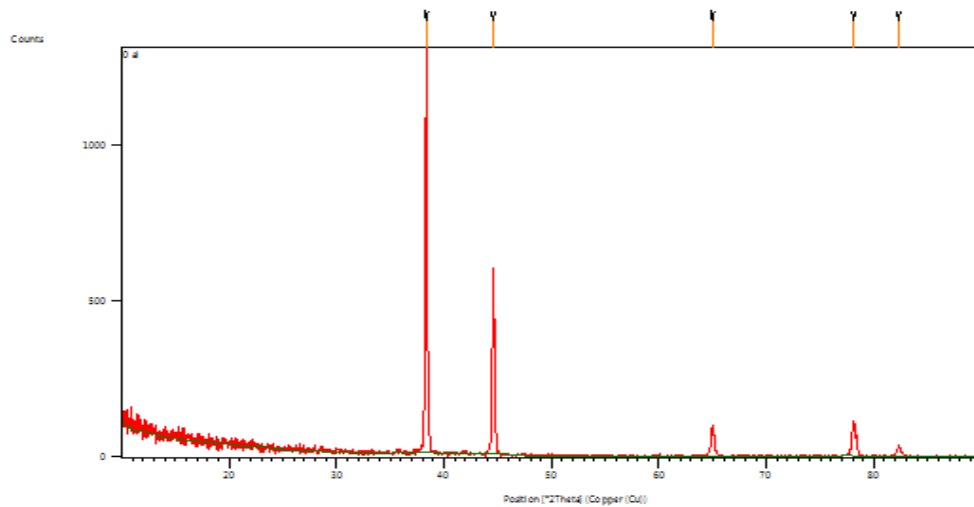
Figure 3.2 XRD result of Al7075

XRD result of the Al7075, shown in fig 3.3 gives the composition of the alloying elements which confirms the values given in table-1.

Table3.2. Physical, mechanical and thermal properties of A7075 alloy [8,29]

Properties	Permanent mould
Density (g/cm^3)	2.81
Ultimate tensile strength (MPa)	225-570
Yield strength (MPa)	89.63
Elongation (% in 2")	8
Shear strength (GPa)	150-350
Brinell Hardness	60
Tensile strength (T)/compressive strength(C) (Mpa)	235

Impact strength (J)	15.2
Modulus of elasticity (GPa)	75
Poisson's ratio	0.33
Fracture Toughness (MPa.$\sqrt{m}$)	22
Thermal Conductivity (W/m.K)	155
Coefficient of thermal expansion (μm/m.K)	21.5
Melting temperature (°C)	475- 635

3.3 FILLER MATERIAL

Ceramic matrix composites (CMCs) are finding increased application in high temperature areas in which metal and polymer matrix composites cannot be used. This is not to say that CMCs are not attractive otherwise, especially considering their high strength and modulus, and low density. In the present work in development of composites Garnet, Flyash and graphite are used as a filler in the different sets of composite in different percentages. The compositions of the different fillers are shown in table 3.3. Different percentages of fillers in different composites are shown in table 3.4.

Table 3.3 Compositions of (a) Garnet (b) Flyash

(a)

Garnet[$Ca_2Al_2(SiO_4)_3$] Composition		
Silica	Alumina	Lime
40.0	22.7	37.3

(b)

Fly Ash Composition								
Al_2O_3	SiO_2	MgO	Fe_2O_3	TiO_2	CaO	Na_2O	K_2O	Lol
30.40	54.41	1.86	7.44	1.75	1.6	1.1	2.1	1.6

Garnet, fly ash and graphite fillers are used in particle form of size 75-106 μm, 50-75 μm, 90-150 μm respectively. SEM image of the garnet, flyash and graphite fillers are shown in fig 3.3.
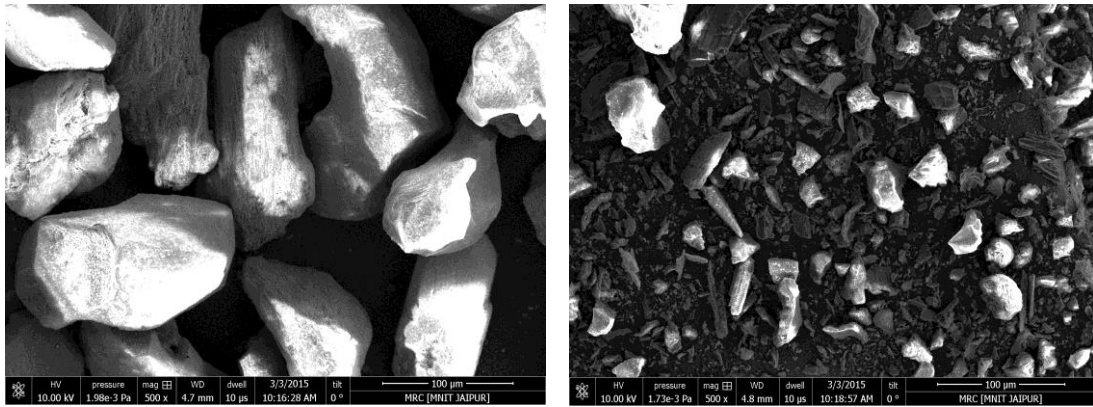
(a)   (b)
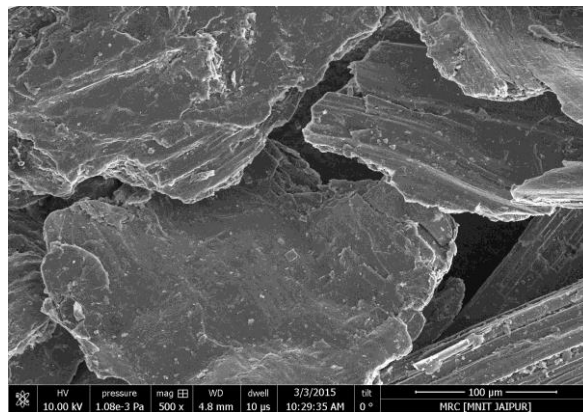
(c)

Figure 3.3 SEM image of (a) Garnet particles (b) Fly ash particle (c)SEM image of graphite particle

SEM results are at 500 times magnification and show the uniform particle size. EDS results of the garnet and flyash particles shows the elemental composition which confirms the values shown in table 3.3. Different properties of the filler materials are presented in table 3.3.
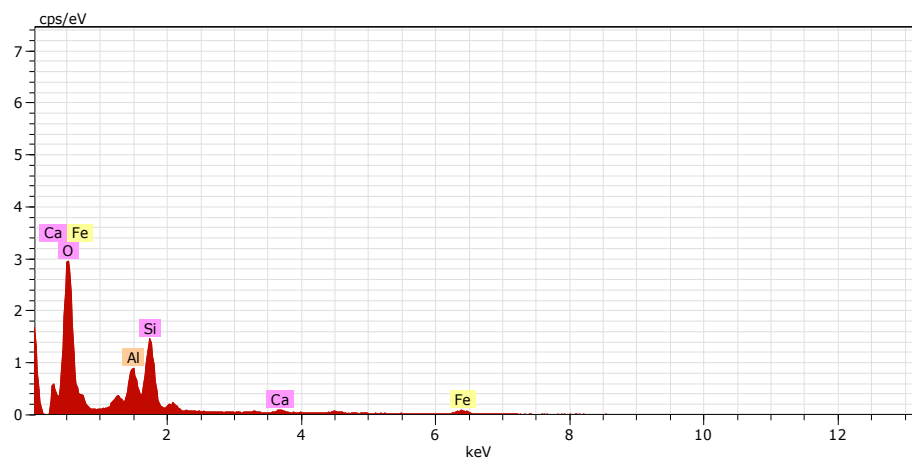
(a)
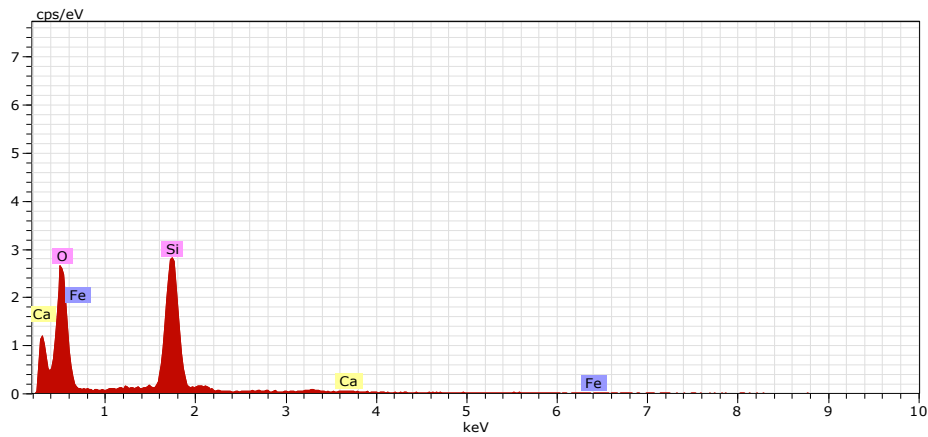
(b)

Figure 3.4 EDS results of (a) Garnet particles (b) Flyash particles

Table 3.3. Properties of Garnet, Fly Ash and Alumina [46,50,51,]

Properties	Garnet	Fly Ash	Graphite
Density (g/cm^3)	3.9-4.1	2.1 to 3.0	2.26
Tensile strength (MPa)	280	275-700	14-34
Young's Modulus (GPa)	282	143–310	1000
Poission's ratio	0.28	0.22	0.16-0.17
Mohs Hardness	8.0 - 9.0	9	1.0 - 2.0
Thermal-conductivity (W/m.K)	12.9	0.06–0.16	510
Melting temperature (°C)	1200	>1200	3500

3.3 FABRICATION TECHNIQUE

3.3.1 Double stir casting

A recent development in stir casting process is a double stir casting or two-step mixing process. In this process, first the matrix material is heated to above its liquidus temperature. The melt is then cooled down to a temperature between the liquidus and solidus points to a semi-solid state. At this point the preheated reinforcement particles are added and mixed. Again the slurry is heated to a fully

liquid state and mixed thoroughly. In double stir casting the resulting microstructure has been found to be more uniform as compared with conventional stirring. The potency of this two-step mixing method is mainly due to its ability to break the gas layer around the particle surface which otherwise impedes wetting between the particles and molten metal. Thus the mixing of the particles in the semi-solid state helps to break the gas layer because of the abrasive action due to the high melt viscosity [30-35].

3.3.2 Composite preparation

The different sets (table 3.4) of composites are prepared with the help of double stir casting method. The fabrication process involved the melting of matrix material, preheating of fillers, stirring of molten metal and the filler mixture and then pouring of composite mixture in the mould. In fig 3.5 a block diagram of the fabrication process is shown.
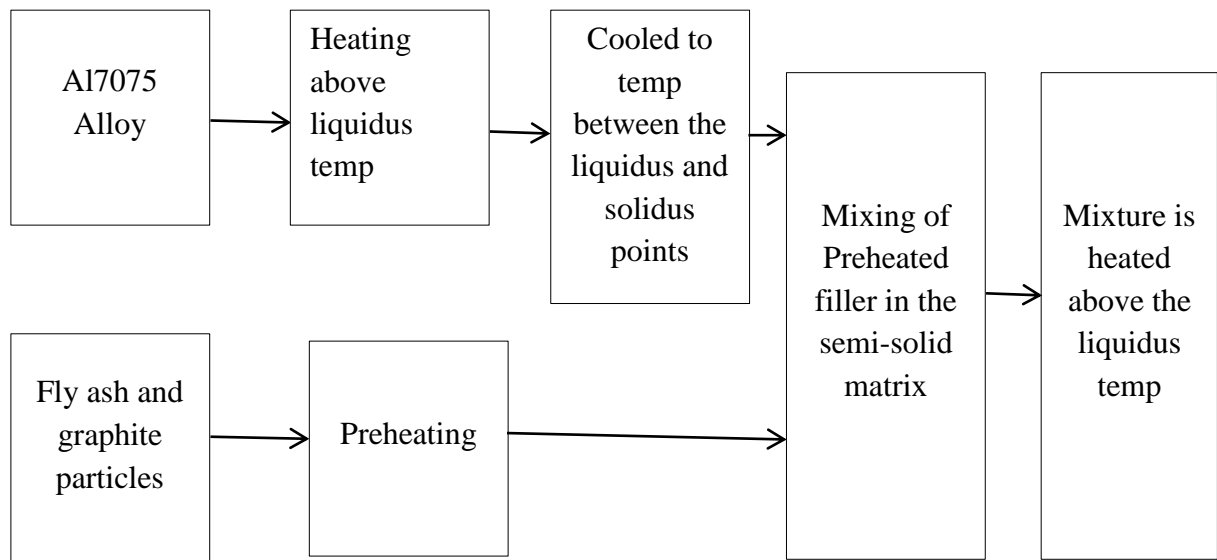
Fig 3.5 Pictorial representation of fabrication of MMC by double stir casting method

Muffle furnace shown in fig 3.6(a) is used for the melting of the matrix material by heating it up to 750^0C and the filler is preheated up to 300^0C in separate furnace. Preheated filler is mixed in the molten matrix material with the help of stirring mechanism shown in fig. 3.6(b). A graphite rode is used as a stirrer. The mixing of filler is done in to steps in first step the mixing is in the semisolid state of the matrix material which is obtained at temperature between 475^0 and 650^0. After the first stage of mixing the mixture again kept in the furnace and heated above the melting point

(750^0C) and then again mixed with the help of stirring mechanism. The different sets of composites developed are shown in table 3.4.

| (a) | (b) |

Figure 3.6(a)Muffle furnace (b)Stirring mechanism

Graphite crucible shown in fig 3.7(a) is used for the casting process and steel mould shown in fig 3.7(b) of dimension 145×90×10 mm is used to obtain a plate of the desired composites.

| (a) | (b) |

Figure 3.7 (a) Molten metal in crucible (b) Fabricated composite plate in mould

Table 3.4 Fabricated composites composition

	Composite	Wt% of Components			
		Al7057	Garnet	Flyash	Graphite
	C0	100	-	-	-
Set 1	C1	95	03	-	02
	C2	92	06	-	02
	C3	89	09	-	02
	C0	100	-	-	-
Set 2	C'1	95	-	03	02
	C'2	92	-	06	02
	C'3	89	-	09	02

3.4 PHYSICAL AND MECHANICAL CHARACTERIZATION

The physical and mechanical characterization of garnet/graphite and flyash/graphite filled Al7075 alloy composites are discussed under the following section.

3.4.1 Density and void content

The theoretical density and void content of the composites in terms of weight fraction is obtained using the rule of mixture given in equation 3.1 and 3.2 by Agarwal and Broutman [39]. The actual density of the composites was measured by the Archimedes principle of weighing the sample first in air and then in water.

$$\rho_c = \frac{1}{(W_p/\rho_p)+(W_m/\rho_m)} \tag{3.1}$$

Where, w and ρ represents the weight fraction and density respectively. The suffix c, p and m stand for composite, particulate and matrix material respectively.

The actual density of the composite can be calculated experimentally by Archimedes's principle.

$$\text{Void content} = \frac{\rho_{ct} - \rho_{ce}}{\rho_{ct}} \qquad (3.2)$$

Where, suffix ct and ce represents theoretical and experimental values of density.

3.4.2 Hardness

The hardness of the fabricated aluminium alloy metal matrix composite is determined by Rockwell hardness tester machine shown in fig . The smooth surface of the specimens is used for hardness measurements. The specimen is indented by 1/16" steel ball. The minor load of 10 kgf and major load of 100 Kgf is applied to the specimen to obtain Rockwell hardness value at B scale. Red dial on scale B gives directly the measures of hardness.
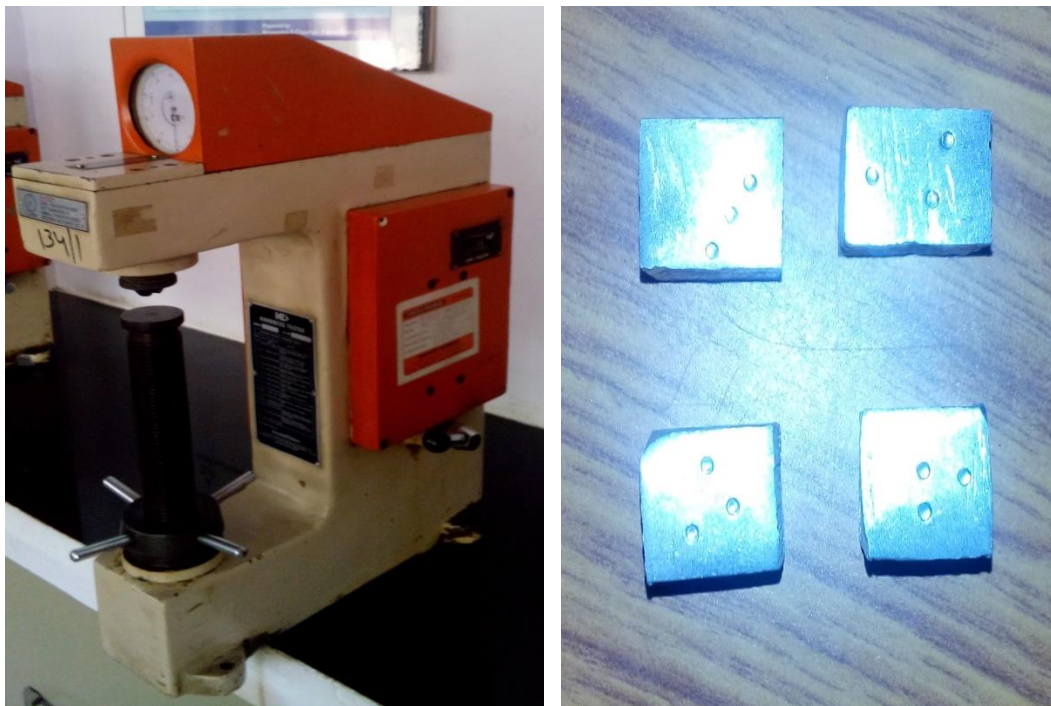
(a) (b)

Figure 3.5 (a)Rockwell hardness testing machine (b)Hardness test specimens

3.4.3 Tensile strength
(a) Experimental

To determine the tensile strength of the composite, a flat specimen is used. The specimens have a rectangle shape with a length, width and thickness equals to 90mmx15mmx4mm, and a spam length of 50 mm. The commonly used specimens for tensile test are the dog-bone type and the straight side type with end tabs. During the

test a uniaxial load is applied through both the ends of the specimen with 2mm/s cross sectional speed. The tensile tests were conducted on a Electronic tensometer (Figure 3.4.) and results are analyzed to calculate the tensile strength of composite samples.

Figure3.6 Specimen for tensile test

ASTM Standard for tensile test specimen (small specimen)

nominal diameter	0.25 ±0.005
Gauge length	1.000±0.005
Fillet radius (min.)	5⁄16
Length of reduced section (min.)	1.25

(All values are in inches)

Figure 3.7 Electronic Tensometer

(b)Theoretical

Tensile strength and elastic modulus are evaluated based on two different theoretical models (i) Series Model (ii) Parallel Model(1)

(i) Parallel Model:

$$T_c = V_m \times T_m + V_{f1} \times T_{f1} + V_{f2} \times T_{f2} \tag{3.1}$$

$$E_c = V_m \times TE_m + V_{f1} \times TE_{f1} + V_{f2} \times TE_{f2} \tag{3.2}$$

(ii) Series Model:

$$T_c = \frac{(T_m \times T_{f1} \times T_{f2})}{(T_{f1} \times T_{f2} \times V_m) + (T_m \times T_{f2} \times V_{f1}) + (T_m \times T_{f1} \times V_{f2})} \tag{3.3}$$

$$E_c = \frac{(E_m \times E_{f1} \times E_{f2})}{(E_{f1} \times E_{f2} \times V_m) + (E_m \times E_{f2} \times V_{f1}) + (E_m \times E_{f1} \times V_{f2})} \tag{3.4}$$

where, T_c, T_m, T_{f1} and $T_{f2}$are the tensile strength of composite, matrix and two fillers and V_m, $V_{f1}$and $V_{f1}$are the volume fraction of matrix and two fillers.E_c, E_m, E_{f1} and $E_{f2}$are the Young's modulus of composite, matrix and two fillers respectively.

(c) FEM Model

The tensile strength of particulate filled metal alloy matrix is studied both experimentally and by finite element analysis. To find the tensile strength with the help of FEM model a standard size specimen is drawn in the ANSYS then solved for defined load and boundary conditions.
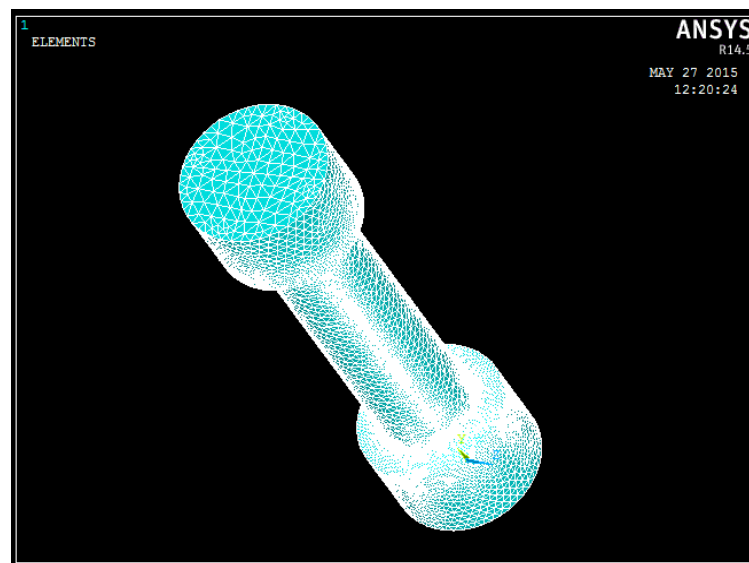
Figure 3.8 Meshed specimen for stress analysis

3.4.4 Impact strength

The Charpy impact test is performed on the test specimen using impact testing machine. A notched sample is used to determine impact strength. The test is done as per ASTM D 256 standard. The standard specimen used is 55 mm × 10 mm ×10 mm. The specimen is placed in the specimen holder as a simply supported beam with the notch facing opposite to the hammer. The hammer is made to strike the specimen at an angle of 120°. The pendulum impact testing machine ascertains the notch impact strength of the material by shattering the V-notched specimen with a pendulum hammer, measuring the spent energy, and relating it to the cross section of the specimen. The value of impact energy is read directly by the dial indicator.

(a)   (b)

Figure 3.8(a)Impact testing Machine (b)Impact test specimen

3.4.5 X-ray diffraction pattern

X-ray diffraction (XRD) is a non-destructive technique and is used for the characterization of crystalline materials. The method is used for phase identification, quantitative analysis and for the determination of structure imperfections. A sample size of 20mm × 15mm × 1mm is prepared for analysis. The surface of the sample is smoothened before placing it in the sample holder. The sample is pressed into a sample holder so that we have a smooth flat surface. The composition of the Al alloy was verified by X-ray diffraction testing. (Fig.3.9)

Figure 3.9 X-ray diffraction testing machine

3.4.6 Scanning electron microscope

Scanning electron microscope (SEM) is used for the study of the worn surface. SEM is capable of generating image of nanometer levels and at different pressure and temperature conditions. Image of surfaces are generated with the help focused electrons which generates signals on interacting with atoms. A sophisticated set up of the SEM is shown in fig. 3.9.

Figure 3.9 SEM test set-up

3.5 WEAR CHARACTERIZATION

3.5.1 Experimental setup for wear testing

Wear testing is performed on the reciprocating tribometer. The wear tests are performed at a normal load of 2 N, 4 N, 6 N and 8 N against EN32 steel plate of hardness RC65. The surface of both the specimens and the steel plate is polished using emery paper (2000grit size) prior to each test. Initial weight of the specimen is weighed using electronic balance having an accuracy of 0.1 mg. The k type thermocouple is attached in the specimen near the contact surface. A vibrometer is fitted on top of the specimen, in turn which is connected to the transmitter and the receiver is connected with the computer. Wireless Vibration Acquisition System integrated with MATLAB software is used to record the time versus amplitude plot during the test. Friction forces are measured from force transducer whichis placed under the steel plate. After the test the final weight of the specimen is measured. Themass loss of the specimen is calculated by finding the difference betweenthe initial weight and final weight. The measured values ofmass loss for all the specimens tested were converted into volumeloss using measured density of the alloy. The mass loss of the specimenwas used to study the effect of particle addition, load on thewear resistance of the composite materials. The worn surfaces of the samples were examined using SEM.
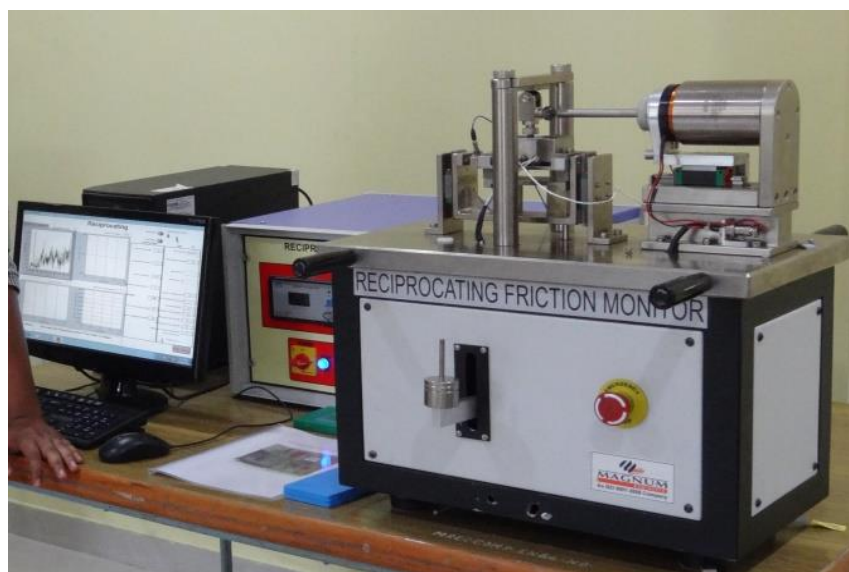

Fig 3 Reciprocating friction monitor

3.5.2 Design of Experiments (DOE)

Design of Experiment is one of the important and powerful statistical techniques to study the effect of multiple variables simultaneously and involves a series of steps which must follow a certain sequence for the experiment to yield an improved understanding of process performance as reported by Taguchi G (1990). All designed experiments require a certain number of combinations of factors and levels be tested in order to observe the results of those test conditions [77]. The DOE process is made up of three main phases: the planning phase, the conducting phase, and the analysis phase. A major step in the DOE process is the determination of the combination of factors and levels which will provide the desired information reported by Fisher R.A.(1951).Taguchi techniques have been used widely in engineering design. This method is useful for studying the interactions between the parameters, and also it is a powerful design of experiments tool, which provides a simple, efficient and systematic approach to determine optimal process parameters. Compared to the conventional approach of experimentation, this method reduces drastically the number of experiments that are required to model the response functions. Taguchi has used Signal–Noise (S/N) ratio as the quality characteristic of choice. The plan of experiments is generated in Taguchi method by the use of standard orthogonal arrays. The experimental results are then analyzed by using analysis of mean and analysis of variance (ANOVA) of the influencing factors reported by Taguchi G et. al.(1987)[90] and Taguchi G (1990)[90].

The Taguchi method is a commonly adopted approach for optimizing design parameters. The method is originally proposed as a means of improving the quality of products through the application of statistical and engineering concepts. Since experimental procedures are generally expensive and time consuming, the need to satisfy the design objectives with the least number of tests is clearly an important requirement. For the elaboration of experiments plan the method of Taguchi for five factors at four levels is used, being understood by levels taken by the factors. In Table 2is indicated the factors to be studied and the assignment of the corresponding levels. The array chosen was the L16 (4^5) which has 16 rows corresponding to the number of tests with 13 columns at three levels, as shown in Table 3the factors and the interactions are assigned to the columns.

In practice, these factors can be assigned arbitrarily to any of the arrays columns, provided that all combinations are included. After assigning appropriate level settings, the S/N analysis (S/N: signal to-noise ratio) is needed to evaluate experiment results. In S/N analysis, the greater the S/N, the better the experimental results:

$$\eta = -10 \log (M.S.D.) \tag{1}$$

where M.S.D. is the mean-square deviation for the output characteristic (specific wear rate). As mentioned earlier, there are three categories of quality characteristics, i.e. lower-the-better, higher-the-better, and nominal-the-better. To obtain optimal performance, lower-the-better characteristic for wear rate must be taken. The mean-square deviation (M.S.D.) for the lower-the-better characteristic can be expressed as [86]:

$$M.S.D. = \frac{1}{m} \sum_{i=1}^{m} T_i^2 \tag{2}$$

where m is the number of tests and Ti is the value of experimental result of the ith test. Furthermore, a statistical analysis of variance (ANOVA) is performed to identify the process parameters that are statistically significant. With the S/N and ANOVA analyses, the optimal combination of the process parameters can be predicted to a useful level of accuracy. Finally, a confirmation experiment is conducted to verify the optimal process parameters obtained from the parameter design [80-87].

Chapter summary

This chapter provides details about:

1. The descriptions of matrix and reinforced material used in the experiments.
2. The details of fabrication and characterization method for composites.
3. The description of theoretical, experimental and finite element method used for the calculation of mechanical properties and fracture toughness.
4. The description of reciprocating wear test.
5. The description of Taguchi Method.

The next chapter discusses the physical, mechanical and fracture behavior of fabricated composite.

*****

MECHANICAL CHARACTERIZATION OF THE FABRICATED COMPOSITES

4.1 INTRODUCTION

This chapter presents the physical and mechanical properties of the ceramic reinforced Al7075 alloy composites prepared for present study. The interpretation of the results and the comparison among various compositions of fillers are also presented. This chapter deals with characterization of two different sets of composites, one for the Garnet/Graphite particulate filled composites (C_0, C_1, C_2 & C_3) and the other for the Flyash/Graphite particulate filled composites (C'_0, C'_1, C'_2, & C'_3).

4.2 DENSITY AND VOLUME FRACTION OF VOIDS

The experimental density of Garnet/Graphite filled Al7075 alloy composites are determined using Archimedes principle and compared with the theoretical results as shown in Table 4.1. It is observed that with increase in filler content, the void content in the composite also increases. The magnitudes of experimental density remain comparatively lower than the theoretical density. This may be attributed to the fact that theoretical results are based on idealistic assumptions that differs experimentally. However, the reinforced composites shows higher density then the unreinforced Al7075 alloy composite and further it increases with increase in garnet content.

Table 4.1 Void fraction

Composites System	Theoretical Density (gm/cc)	Experimental Density (gm/cc)	Void fraction (%)
C0	2.81	2.7895	0.726
C1	2.8199	2.795	0.88
C2	2.8438	2.8157	0.987
C3	2.8681	2.8333	1.210
C'1	2.7861	2.7603	0.923
C'2	2.7758	2.7445	1.125
C'3	2.7656	2.7282	1.351

However, in stir casting, it is difficult to avoid void content as it is an unavoidable parameter in case of particulate filled composites. The amount of porosity and density in the composites is found to increases with the increase in weight fraction and decrease in size of the particles. In this study, the pressure immediately applied after the casting, has reduced the porosity in the composites, and improved the bonding force between the Al alloy and filler materials. Similar, observations was observed for 2024 aluminum alloy metal matrix composites with Al_2O_3 filler particles, the density of the composites increased with increasing weight percentage and size of particles, whereas, the porosity of the composites increased with decreasing in size and increasing the weight percentage of particles [25].

4.3 HARDNESS

The variation of hardness with respect to Garnet and flyash filler contents in A7075 alloy composite is shown in fig.4.1 and fig.4.2. The hardness of the composites increases more or less linearly with the increased in the weight fraction of filler particle in Al7075 alloy composites. This may be attributed to presence of harder ceramic phases then the Al7075 alloy phases in the composite. The maximum value of hardness at 9wt.% Garnet is found to be 88 HRB. As hardness is a measurement of resistance of the material to indentation under standard conditions, the resistance of the material is actually localized plastic deformation. The increase in hardness is quite obvious and expected since Garnet is a hard dispersoid and contributes positively to the hardness of the composites. The increase in hardness with increase in weight percent of filler particles is mainly due to grain refinement and particle strengthening effects.
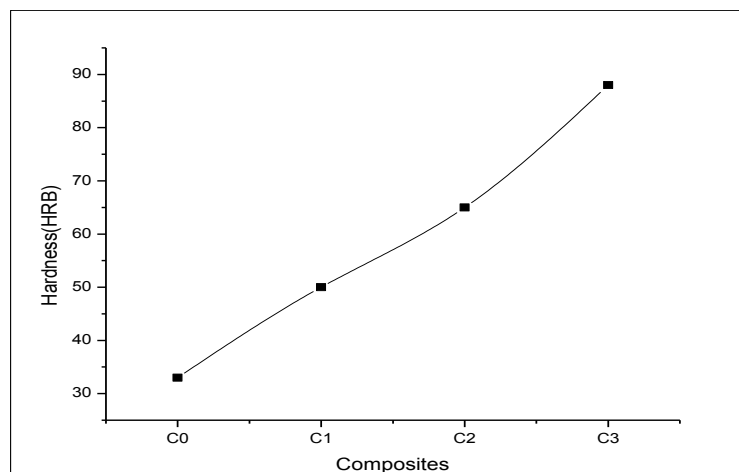

Figure 4.1 Variation in harness with garnet filler percentage
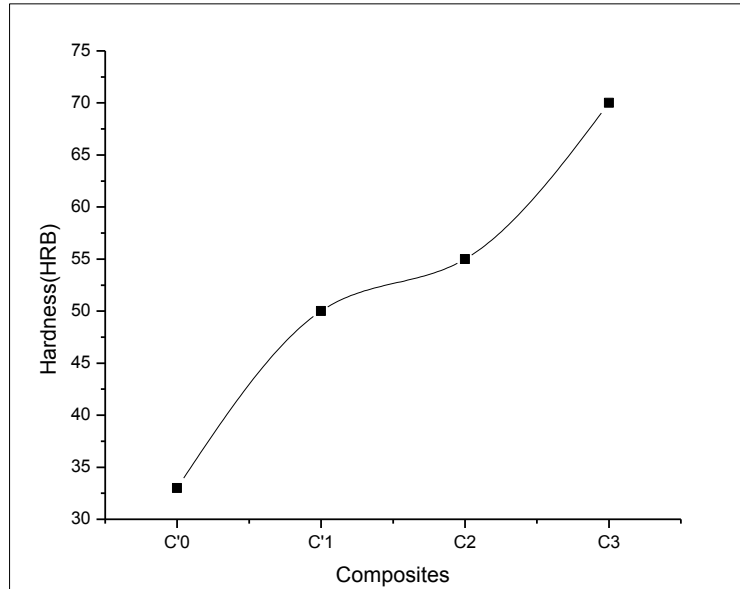
Figure 4.1 Variation harness with flyash filler percentage

4.4 TENSILE STRENGTH

The tensile strength at different fabricate Al7075 alloy composites has been studied experimentally, theoretically and by finite element analysis. The results for tensile strength of Garnet/Graphite and Flyash/Graphite filled Al7075 alloy composite are shown in Figure 4.3 and Figure 4.5 respectively. From Figure 4.1, it is observed that the FEM results for tensile strength for Garnet/graphite filled Al7075alloy composites are slightly higher than the experimental results but within the acceptable domain. The theoretical values of tensile strength calculated are showing deviation from Experimental and FEM results which is due to the presence of graphite particles. It is observed that the FEM results and experimental results are in close approximation to each other and the result converges at higher wt.-% of reinforcement. As the weight fraction of the ceramic particles increases, the transfer of load to the reinforcement also increases thus resulting in higher ultimate tensile strength. The work hardening rate increases with the increasing weight fraction of the reinforcement. The lower ductility can be attributed to the earlier onset of void nucleation with the increasing in amount of reinforcement. However, particle clustering has a significant effect on the ductility of the composites, if the particle fracture is included in the simulation. Therefore, smaller the size of the reinforced particle, higher is the tensile strength. The similar results are also found for flyash/graphite filled Al7075 alloy composite shown fig. 4.5.
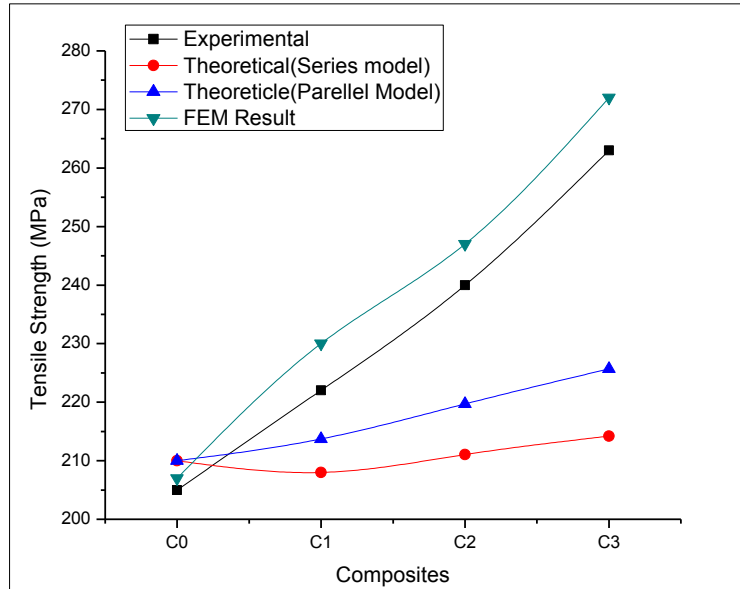
Figure 4.3 Variation in Tensile Strength with garnet filler percentage

Increase in tensile strength with increase in ceramic filler content also observed by Aruria et al. [38]. Authors investigated (SiC + Gr) and (SiC + Al2O3) filled Al6061 hybrid composites and found the increasing trend of Tensile strength with increase in filler content and the increase was more in (SiC+Al2O3) filled composites. The presence of graphite decreases the tensile strength. The similar observation is done by S. Rajesh et al. [107]. S.C. Sharma [29] also investigated the effect of garnet filler on the aluminium matrix and found increase in the tensile strength with garnet filler. Kiran et al.[109] investigated effect of particle size of garnet. They fabricated to sets of composites with three different size of garnet filler(50μm, 75 μm, 150 μm). They found better results for smaller particle size garnet reinforcement.
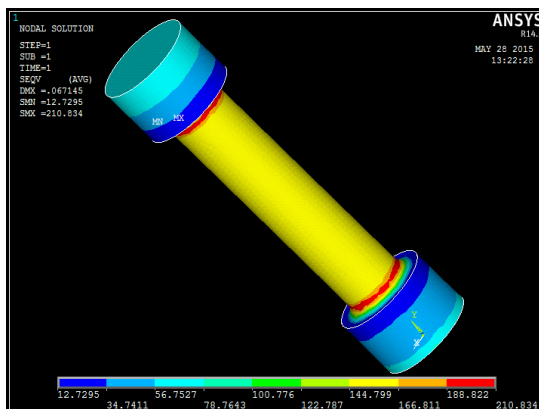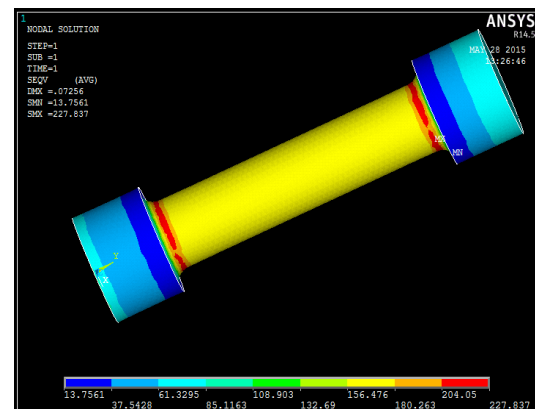
(a)   (b)
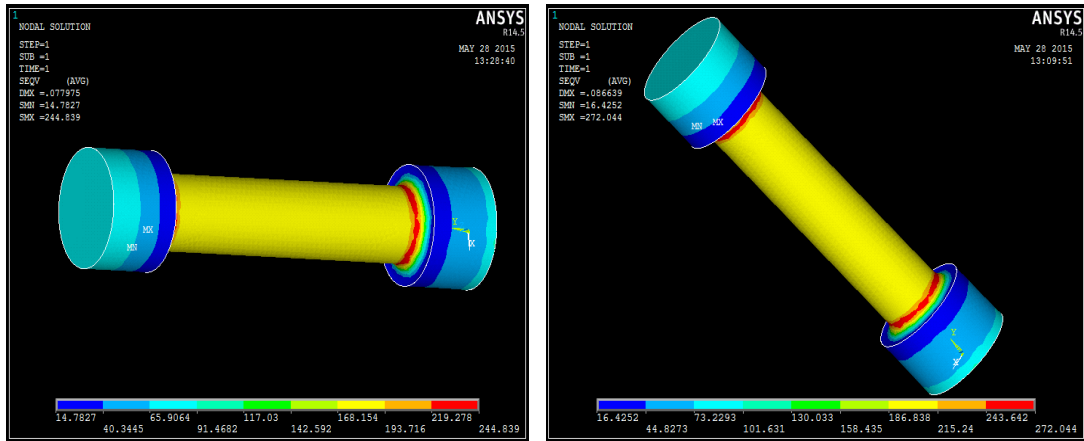
(b)   (d)

Figure 4.4 Results of Von-mises stress in Tensile test by FEM simulation for specimen (a)C0 (b)C1 (c)C2 (d)C3

Tensile test specimen model is designed according to the ASTM standards same as used for the experimental work. Specimens are given the of young modulus value from the experimental result of the individual specimens. Different specimens are given different maximum load which is noted from experimental result of that specimen. So here the developed stress is observed with help of ANSYS von-mises stress simulation. The FEM results for first set of composites shows good association with the experimental results.
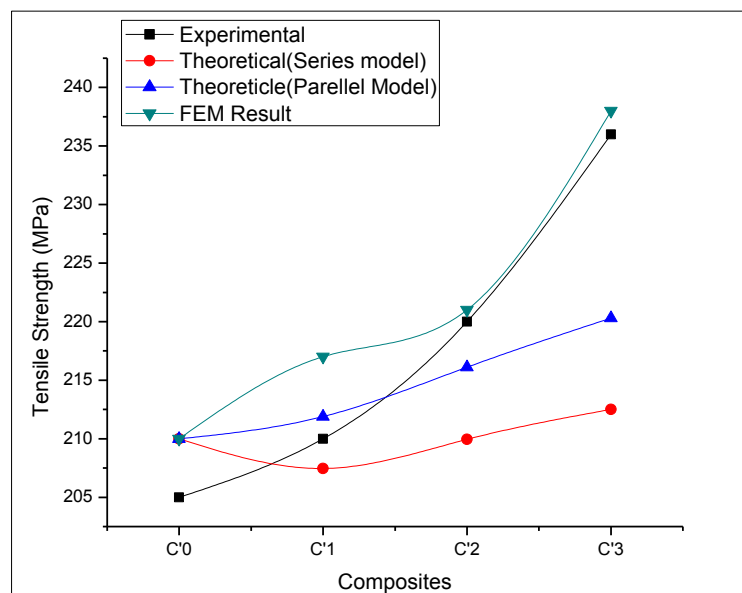
Figure 4.5 Variation in Tensile Strength with flyash filler percentage
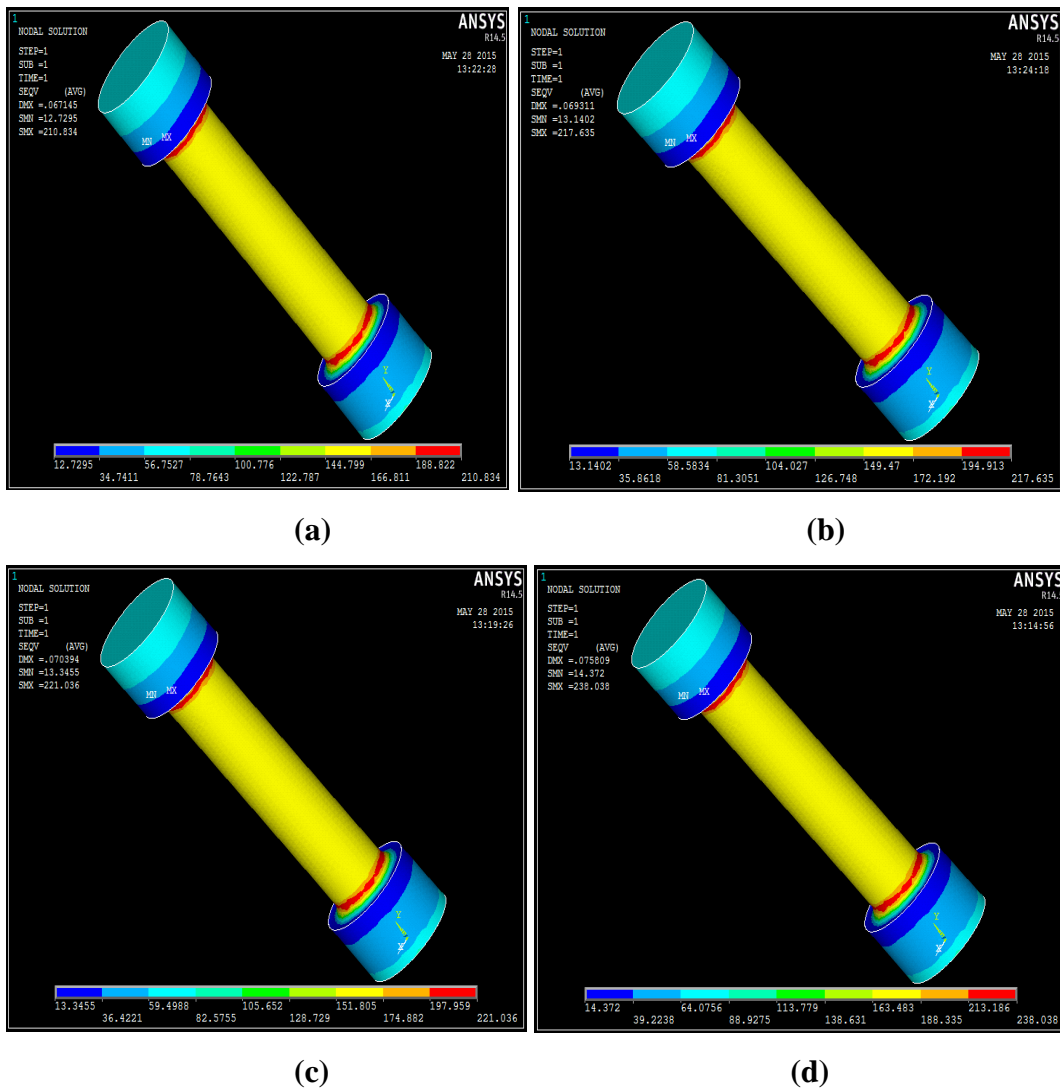
Figure 4.6 Results of Von-mises stress in Tensile test by FEM simulation for specimen (a)C'0 (b)C'1 (c)C'2 (d)C'3

The same simulation is done for second set of the composites based on experimental results. FEM results for the second set of composite does not show very good agreement with experimental results it is due to presence of fly-ash particles.

4.5 MODULUS OF ELASTICITY

Modulus of elasticity of different fabricated composites determined experimentally and theoretically. Young's modulus of the composites increases with the increased wt.-% of filler content for both of the sets of composites. In the two theoretical models the parallel model gives closer results to the experimental values. The same trend is also observed by number of other researchers worked on ceramic filled aluminium matrix composites [40-44]. This increase in the elastic modulus is due to the semi ductile behavior of the composite which is also discussed by Kumar et al. in

his investigation of situ Al–7Si/TiB2 particulate composites mechanical and wear behavior. The increase in first set of composites are more than that of for second set of composites which is due to presence of the harder garnet particles as compare to flyash.
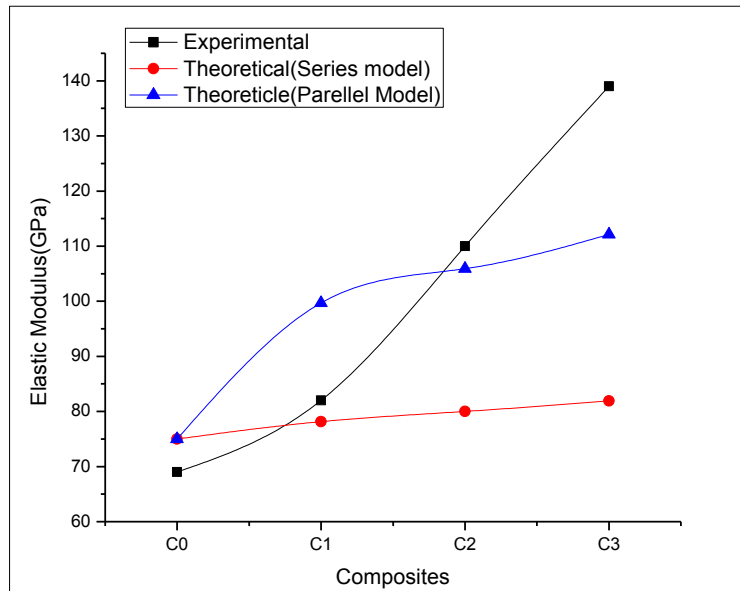
Figure 4.7 Variation of elastic modulus with garnet filler percentage
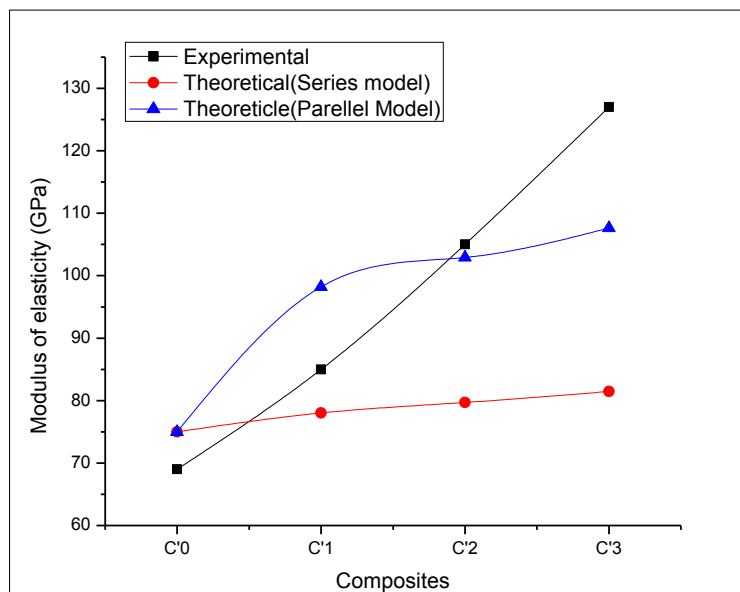
Figure 4.7 Variation of elastic modulus with flyash filler percentage

4.6 IMPACT STRENGTH

The impact energy of fabricated composites in terms of the energy absorbed during Chapy impact test is shown in Figure 4.7 and 4.8. The impact strength (in terms of

impact energy absorbed in Joules during the Charpy impact test) of fabricated composites decreases with the increased wt.-% of filler content for both the sets of composites. And this decrease in the impact strength was due to increase in void content with increase in percentage of filler content. More decrease in impact strength is observed for second set of composites i.e. flyash/graphite filled Al7075 alloy composites.
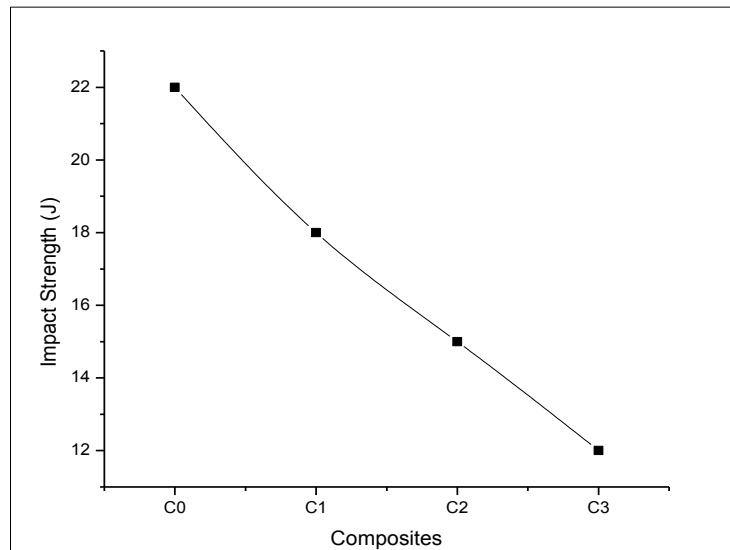
Figure 4.7 Variation of Impact Energy with garnet filler percentage
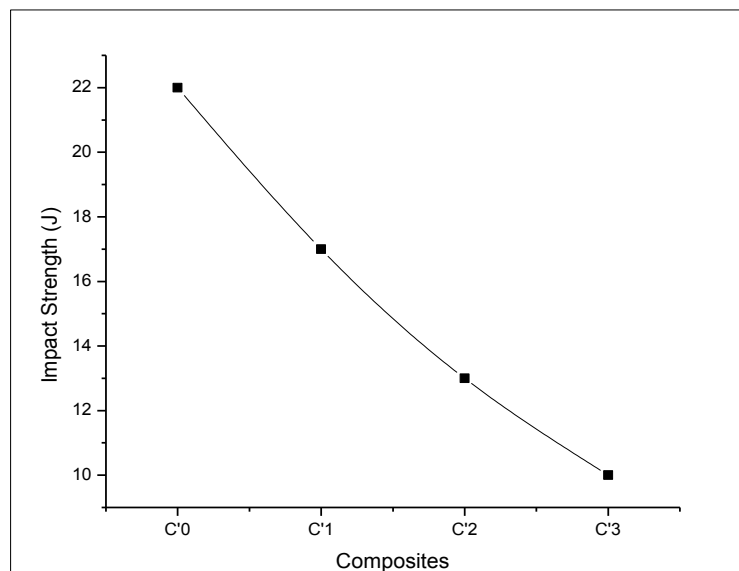
Figure 4.8 Variation of Impact energy with garnet filler percentage

Chapter Summary

Based on the above results the following conclusions are drawn:.

1. Void fraction increases with increase in filler content in Al7075 alloy.
2. Tensile strength, hardness and elastic modulus increases with increase in the filler content for both set of composites.
3. Impact strength decreases with the increases in the filler content.

The next chapter discusses the wear behavior and optimization of wear parameters of fabricated composites.

<p align="center">*****</p>

WEAR BEHAVIOUR OF FABRICATED COMPOSITES AND OPTIMIZATION OF WEAR PARAMETERS

This chapter presents the results obtained from steady state reciprocating wear test and wear parameters optimization of fabricated composites. Steady state wear tests are performed at different operating conditions such as filler content, load, sliding velocity, temperature etc. Finally, the wear of the different composites are comparatively presented with the help of bar diagram. Taguchi method is used to optimize the parameter affecting the wear of specimen.

5.1 THEORETICAL WEAR MODEL

It was observed that wear rate mainly dependent on Hardness, Load, Sliding velocity and Sliding distance. According to the classic Archard's model [34],in equation 6.1 the wear-rate of a material should be inversely related to its hardness. In the present study, there is a general tendency for wear-rate to decrease with increase in hardness. However, the decrease is not linear with hardness of the MMCs. It is clear that the wear-rate of the composites does not correlate well with hardness of the specimen.

$$\frac{dV}{dS} = \frac{KL}{H} \tag{6.1}$$

where dV is the volume of wear debris, L the normal load, dS sliding distance, H the hardness of material and K the wear coefficient, which is usually assumed to be constant.

In the present investigation, it is experimentally observed that the wear rate of fabricated composite is a function of filler content, Load, sliding velocity, sliding distance and temperature. As the temperature has least significance on the wear rate so it can be removed from the final formula for the wear rate. A wear rate for the both sets of composites can be formulated based on Taguchi analysis as given in equation 6.2 and 6.3 respectively.

W = 0.0305131 - 0.0026207 A - 0.0030334 B - 0.00177425 C - 0.00186845 D

-0.0008244 E $\tag{6.2}$

W = 0.030845 - 0.002524 A - 0.002499 B - 0.001727 C - 0.0021695 D -

0.0011075 E $\tag{6.3}$

where W is the wear rate, A the filler content, B the normal load, C the sliding velocity and D the sliding distance.

5.2. STEADY STATE WEAR FOR AL7075 ALLOY COMPOSITES

Steady state wear tests are conducted with variation of one variable at a time while keeping others variables constant. Response curves of wear rate are plotted against variables. It was observed that wear rate mainly dependent on Hardness, Load, Sliding velocity and Sliding distance. And from the experimental results the trend of the variation of the wear rate was revealed that shows the wear rate is inversely proportional to the filler content which was due to presence of ceramic filler particle.

5.2.1. Effect of load on Al7075 alloy composites

The steady-state wear rates are measured at four different loads (2, 4, 6 & 8N) while keeping sliding velocity(0.12 m/sec), sliding distance(180m) and temperature(75^0C) constant. The experimental results of the wear rates for the composites related to the different load are shown in Figure 5.1. It is seen from the figure that the mass loss of the composites is lower than that of the unreinforced Al7075 alloy composites with the similar experimental conditions. A significant increase was observed in wear rate with increase in load. However, among the garnet/graphite and flyash/graphite filled Al7075 alloy composites the minimum wear rate observed for 9%garnet with 2% graphite filled composite.
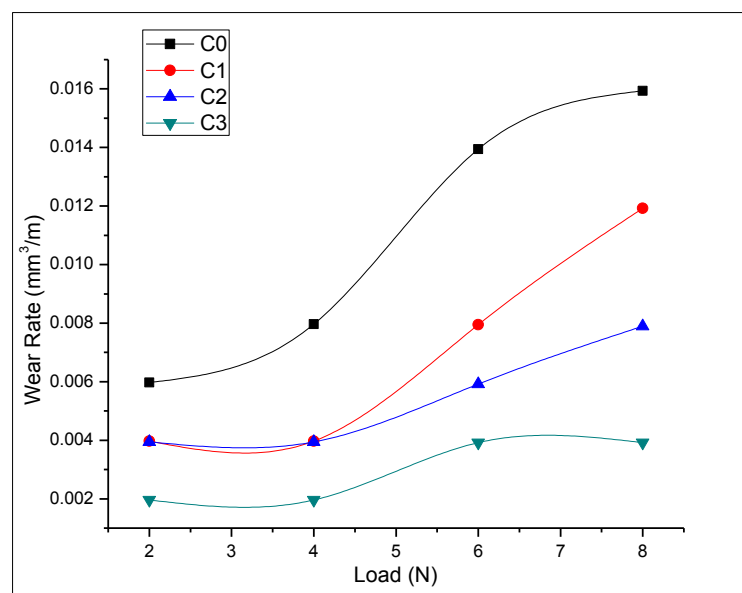
Figure 5.1 Variation of wear rate with load for garnet/graphite filled Al7075 composites.

The fig 6.1 also shows that there is a sudden increase in the wear-rate at a particular applied load, i.e. a transition phenomenon. This transition phase can be seen after the load of 4N but it is absent in C_3 composite which is due to the presence of garnet particles.
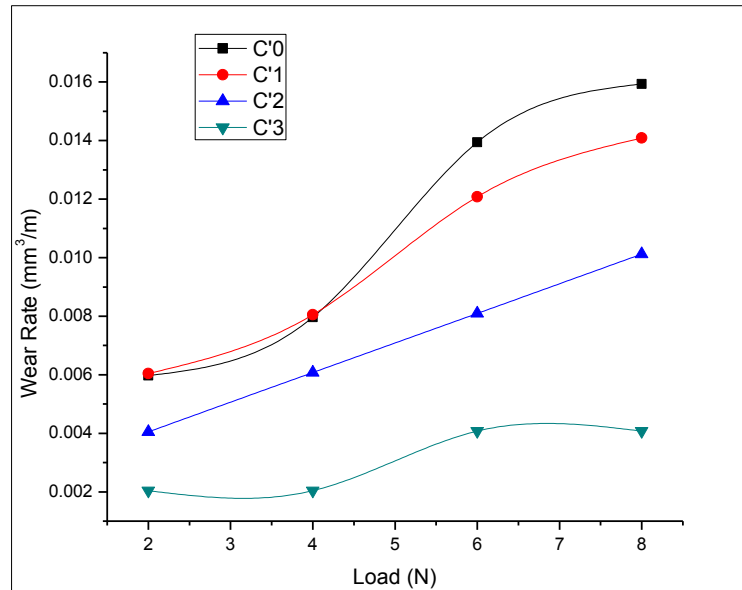
Figure 5.2 Variation of wear rate with load for flyash/graphite filled Al7075 composites.

Similar behavior is also observed for second set of composites from fig 5.2 but here a significant reduction in wear rate is found for the C'_3 composite as compare to C'_2 at higher load.

5.2.2. Effect of sliding velocity on Al7075 alloy composites
The steady-state wear rates are measured at four different velocities (0.04, 0.08, 0.012 & 0.016) and at constant load (6N), sliding distance (180m) and temperature (75^0C) . The experimental results of the wear rates for the composites related to the different velocities are shown in Figure 5.3. Change in velocity affecting the wear rate less as compare to load. With increase in velocity the wear rate is increasing. And due to the presence of ceramic and graphite particle which are harder than the matrix material and also give a self-lubricating effect wear rate reduces.
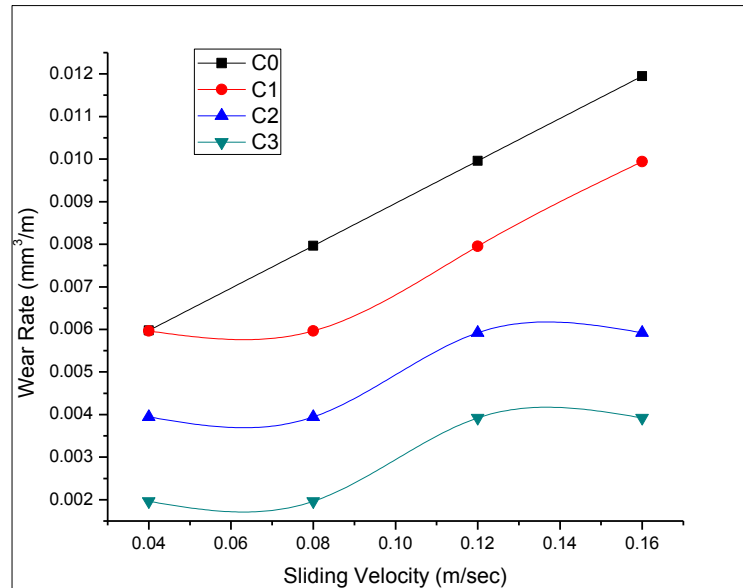
Figure 5.3 Variation of wear rate with sliding velocity for garnet/graphite filled Al7075 composites.

For the similar sliding wear test on pin on disc test rig as the velocity of the test is increased the time for test reduces and higher velocity also promotes the formation of oxide layers which resist the wear of surface. So due to both reduction in test time and formation of oxide layer the wear rate reduces at higher velocity. This is observed by number of researchers [28,30-33]. But in the present investigation it is observed that the wear rate for the composite as well as for unreinforced alloy increases with increase in average velocity. This is due to the reciprocation of specimen. In the reciprocation the velocity does not remain constant but it changes from zero at the extreme points to maximum at the middle of the reciprocation and the acceleration also changes maximum at extremes and zero at middle. This change in velocity and acceleration develops continuous changing inertia force and jerk which is responsible for this increasing wear rate trend with increase in velocity. Increase in wear rate with increase in sliding velocity is also observed the S. C Sharma [63,64]
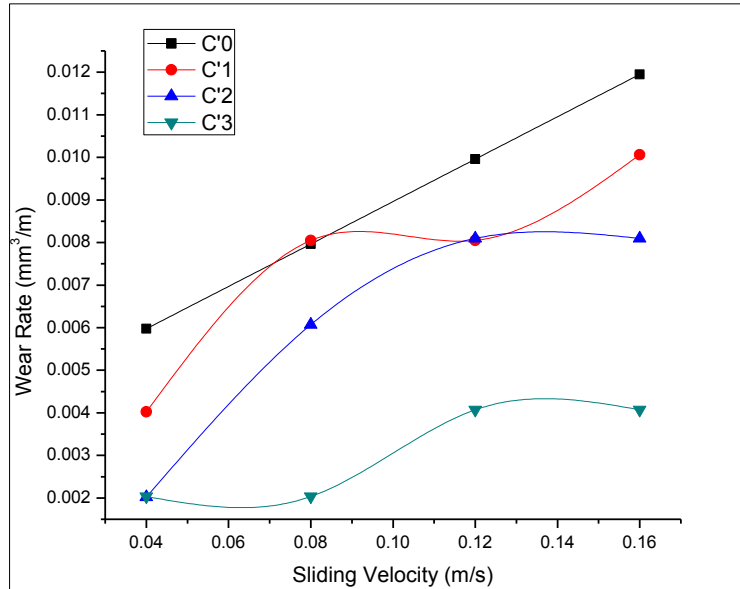
Figure 5.4 Variation of wear rate with sliding velocity for flyash/graphite filled Al7075 composites.

From the fig 5.3 and 5.4 it is observed that the wear rate significantly reduced in the composite with higher percentage of reinforcement i.e. C_3 & C'_3. It is due to the presence of ceramic reinforcement which develops oxide layer at higher velocity.

5.2.3. Effect of temperature on Al7075 alloy composites
The steady-state wear rates are also measured at four different temperature (25,50 & 100^0C). The experimental results of the wear rates for the composites related to the different temperature are shown in Figure 5.3. Change in temperature affecting the wear rate least. A slightly increase observed in the wear with increase in temperature. But in the composite C3 and C'3 the wear rate is almost independent of the temperature.
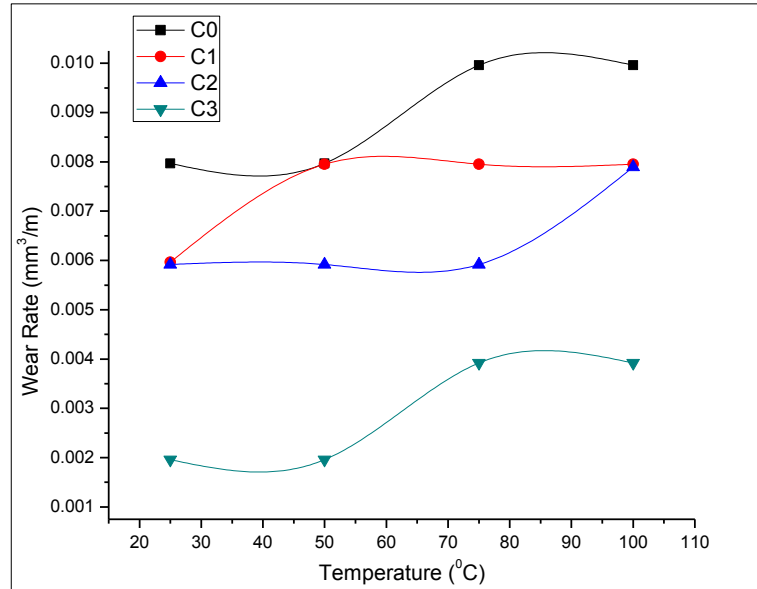
Figure 5.5 Variation of wear rate with temperature for garnet/graphite filled Al7075 composites.
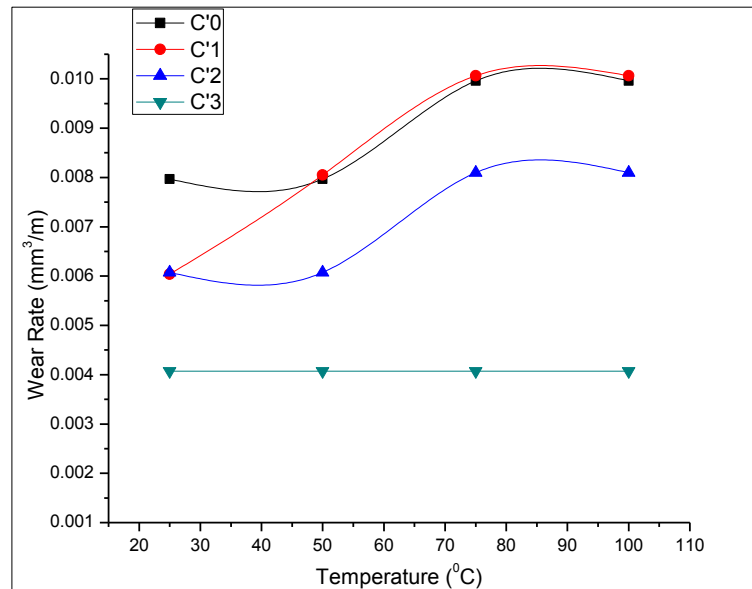
Figure 5.6 Variation of wear rate with temperature for flyash/graphite filled Al7075 composites.

5.3 SURFACE MORPHOLOGY OF WORN SURFACE

Scanning electron microscopic investigation was performed on the worn surfaces. SEM micrographs from both the set of composites are shown in in Fig.5.7 and Fig 5.8 The worn surfaces of the composites show a combined wear pattern, narrow grooves and heavy flow of material along the sliding direction, indicating a greater degree of wear and localized adhesion between the specimen pin surface and the counter body. The wear track can be observed in the images as indicated in fig. 6.7 by the parallel arrows. The dominant abrasive wear mechanism is ploughing, and it is indicated by the worn surface of the topographies of the composites.
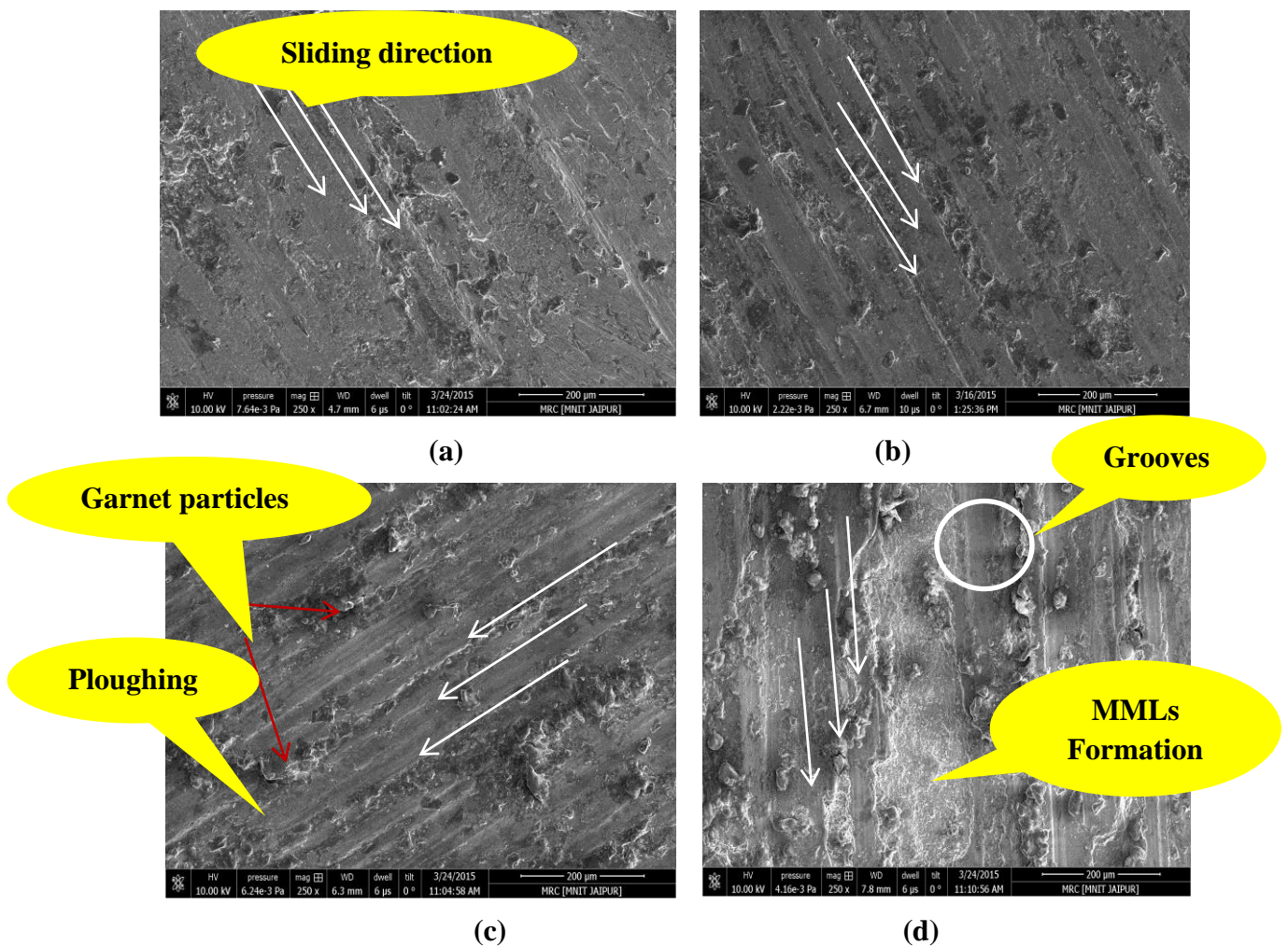
Figure 5.7 SEM micrograph of wear surfaces (a) 0% garnet reinforcement (b) 2% graphite and 3% garnet reinforcement (c) 2% graphite and 6% garnet reinforcement (d) 2% graphite and 9% garnet reinforcement with 8N load for 180m sliding distance

It can be observed from the SEM results clearly that there is a formation of smoother surface in case of unreinforced as compare to the surface generated after wear of composites. It was due to the presence of garnet particles which are much harder than the parent material. These garnet particles prevent the delayering of the contact surface which results in rough worn surface which was not found in softer unreinforced Al-alloy pins. The wear rate of these composites are also less as compare to unreinforced Al-alloy the reason of this is formation of mechanical mixed layer at the wear zone. The same phenomenon observed by S.C. Sharma[29] and Lakshmipathy et al.[8]. The morphologies of the worn surfaces indicate the existence of abrasion and delaminating wear mechanisms in composites.
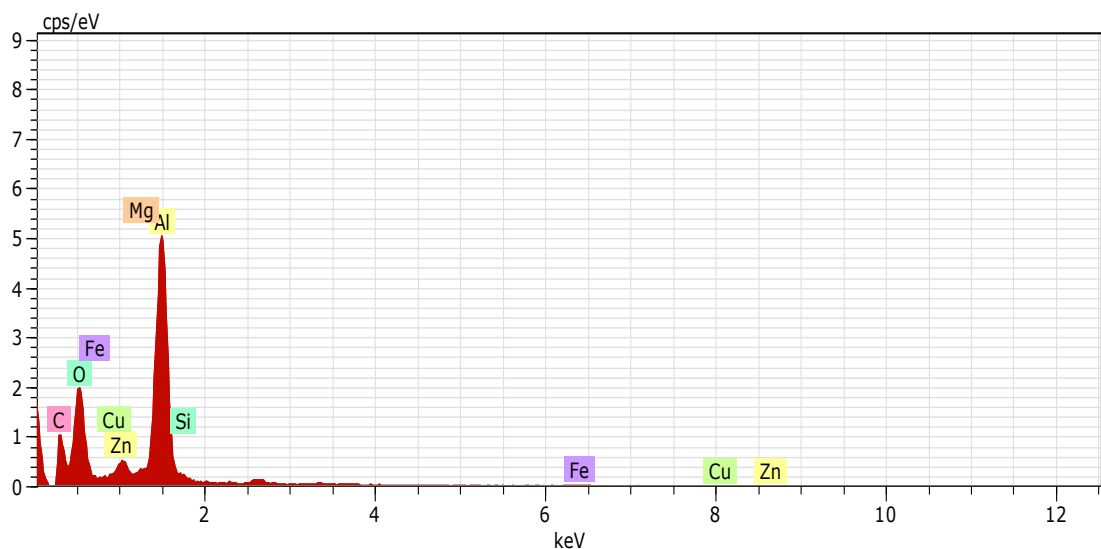
Figure 5.8 EDS spectrum of the worn zone

EDS test is performed to observe the elemental content at the worn surface. Here the presence of mechanical mixed layer(MML) at the worn suface can be confirmed by the EDS results(Oxides of iron and aluminium). Presence of iron at the worn suface is due to the steel counter part sticking on the reciprocating pin. MMLs prevents further delayering of the suface by creating more harder and wear resistant oxide layer of iron and aluminium at worn surface which reson of imroved wear resistance of the composite.
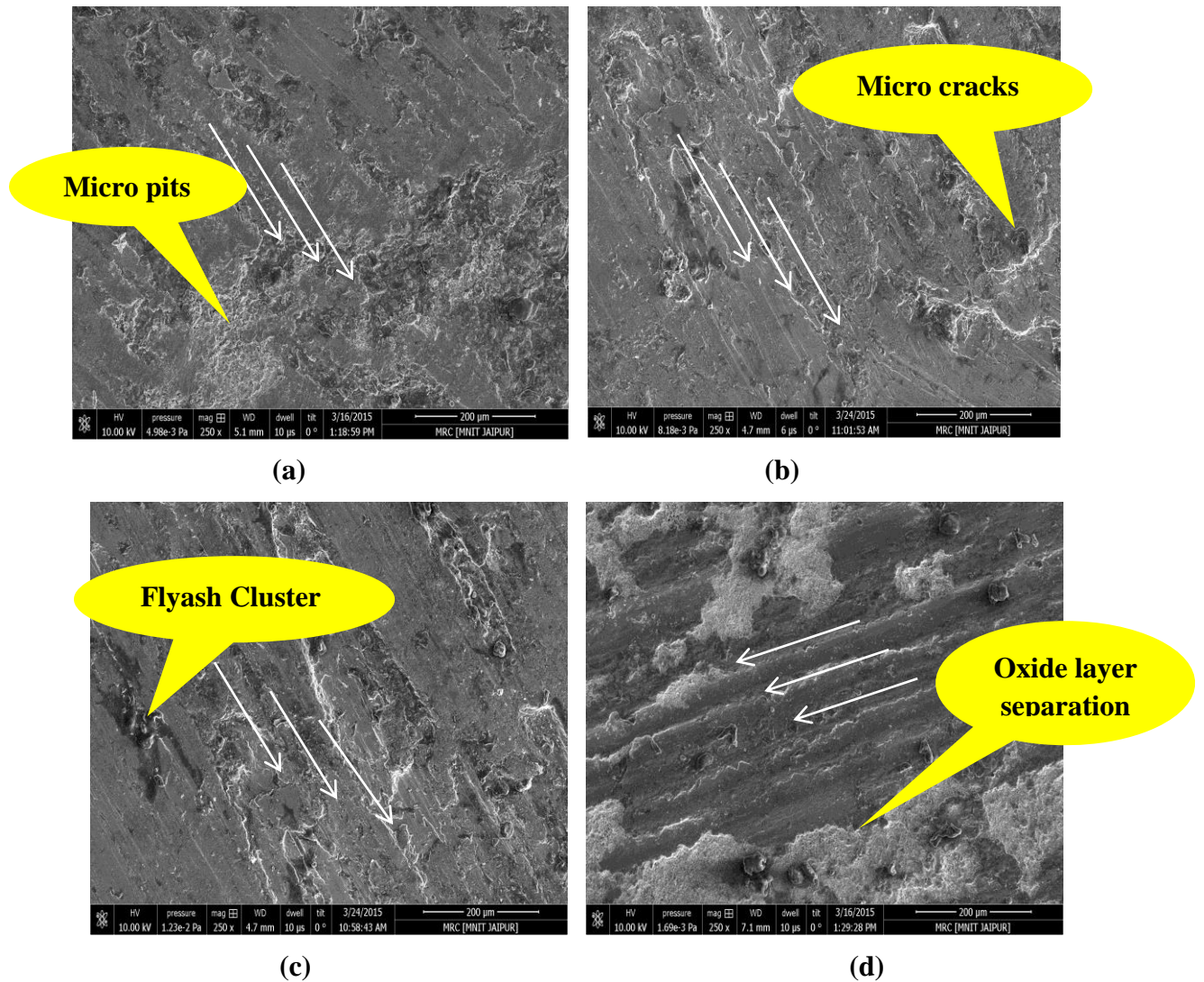
Figure 5.9 SEM images of wear surfaces (a) 0% flyash reinforcement (b) 2% graphite and 3% flyash reinforcement (c) 2% graphite and 6% flyash reinforcement (d) 2% graphite and 9% flyash reinforcement, with 8N load for 180m sliding distance

Smoother worn surfaces are found in the second set of composites i.e. flyash and graphite reinforced composites. There were numerous scratches on wear surface. This suggests that the primary wear mechanisms under these conditions are abrasive wear. Surface projections or asperities present in the contact surface plastically deform and eventually weld together by high local pressure during relative motion between the contact surfaces. As the sliding continues these bonds break up producing microcavities which cause tiny particle abrasion.

5.4 OPTIMIZATION OF WEAR PARAMETERS BY USING TAGUCHI METHOD

5.4.1 Experimental design

Plan of experiments was done using Taguchi's technique and L16 orthogonal array was opted for getting the best results with minimum number of experiments (Table 3). Wear rate of the specimen and the average coefficient of friction were the two responses evaluated using S/N ratio and Analysis of Variance (ANOVA). Experiments were conducted by considering five parameters; percentage reinforcement, applied load, sliding velocity, sliding distance and temperature each of these varied for four levels (Table 5.1).

Table 5.1

Level	Percentage Reinforcement (wt.%)(A)	Applied load (B) (N)	Sliding velocity (C) (m/s)	Sliding distance (D) (m)	Temp (E) (^{0}C)
1	0	2	0.024	20	25
2	3	4	0.036	40	50
3	6	6	0.048	60	75
4	9	8	0.060	80	100

5.4.2 Taguchi analysis

The wear rates of garnet/graphite and flyash/graphite reinforced Al7075 hybrid metal matrix composites under various test conditions are determined experimentally. The experimental observations are transformed into a signal-to noise (S/N) ratios. Table 6.1 and Table 6.2 show the wear rate and S/N ratio of the all the sixteen designed experiments for garnet/graphite filled composites and for flyash/graphite filled composites respectively. The overall mean for the S/N ratio of the wear rate is found to be 49.291db and 47.126db for garnet/graphite filled and flyash/graphite filled composites respectively. Significance of individual factors are shown in fig 5.10 and fig. 5.11 The analysis was made using the popular software specifically used for design of experiment applications known as MINITAB 16. From The S/N ratio response it can be concluded that among all the factors Applied load is the most significant factor followed by filler content, sliding distance and sliding velocity while

the temperature has the least or negligible significance on wear rate of these garnet/graphite filled al7075 alloy hybrid metal matrix composites (Fig 5.10). Effect of individual control factors for signal to noise ratio shown in Fig. 4 also leads to the conclusion that factor combination of A4, B4, C1, D3 and E2 gives minimum wear rate. The reciprocating wear rate was calculated by the following relation:-

$$\text{Wear rate} = \frac{\Delta m}{\rho L V_s t} \tag{6.4}$$

Where Δm is the mass loss in the test duration (g), ρ is the density of the composite (g/mm3), t is the test duration (s), Vs is the sliding velocity (m/s), L is the applied load (N). The specific wear rate is defined as the volume loss of the specimen per unit sliding distance per unit applied normal load.

Table 5.2 Taguchi experiment of first set of composites

Level	A	B	C	D	E	Wear Rate (mm^3/N m)	S/N ratio (db)
1	0	2	0.024	20	25	0.02669	31.47287
2	0	4	0.036	40	50	0.008897	41.01532
3	0	6	0.048	60	75	0.003954	48.05898
4	0	8	0.06	80	100	0.003336	49.53468
5	3	2	0.036	60	100	0.011696	38.63934
6	3	4	0.024	80	75	0.002193	53.17929
7	3	6	0.06	20	50	0.002924	50.68044
8	3	8	0.048	40	25	0.002193	53.17926
9	6	2	0.048	80	50	0.004325	47.27977
10	6	4	0.06	60	25	0.001442	56.82218
11	6	6	0.024	40	100	0.002884	50.8016
12	6	8	0.036	20	75	0.002163	53.30043
13	9	2	0.06	40	75	0.004266	47.3992
14	9	4	0.048	20	100	0.004266	47.39922
15	9	6	0.036	80	25	0.001422	56.94157
16	9	8	0.024	60	50	0.000711	62.96218
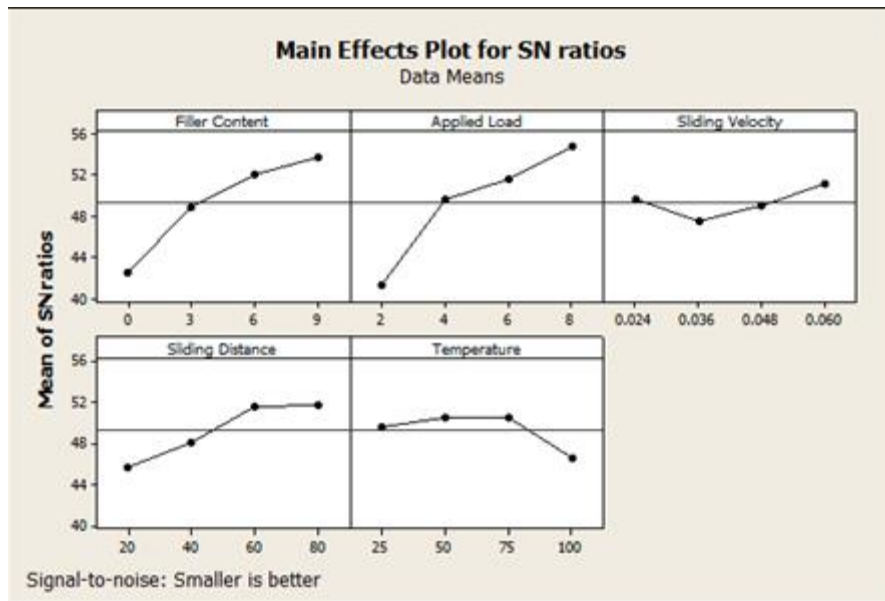
Fig 5.10 Effect of control factors on wear rate (First set of composites)

Table 5.3 Taguchi experiment of second set of composites

Level	A	B	C	D	E	Wear Rate (mm³/N m)	S/N ratio (db)
1	0	2	0.024	20	25	0.0267	31.4729
2	0	4	0.036	40	50	0.0089	41.0153
3	0	6	0.048	60	75	0.00395	48.0590
4	0	8	0.06	80	100	0.00334	49.5347
5	3	2	0.036	60	100	0.00877	41.1381
6	3	4	0.024	80	75	0.00439	47.1587
7	3	6	0.06	20	50	0.00585	44.6598
8	3	8	0.048	40	25	0.00329	49.6574
9	6	2	0.048	80	50	0.00433	47.2798
10	6	4	0.06	60	25	0.00288	50.8016
11	6	6	0.024	40	100	0.00433	47.2798
12	6	8	0.036	20	75	0.00433	47.2798
13	9	2	0.06	40	75	0.00427	47.3992
14	9	4	0.048	20	100	0.00427	47.3992
15	9	6	0.036	80	25	0.00142	56.9416
16	9	8	0.024	60	50	0.00142	56.9416
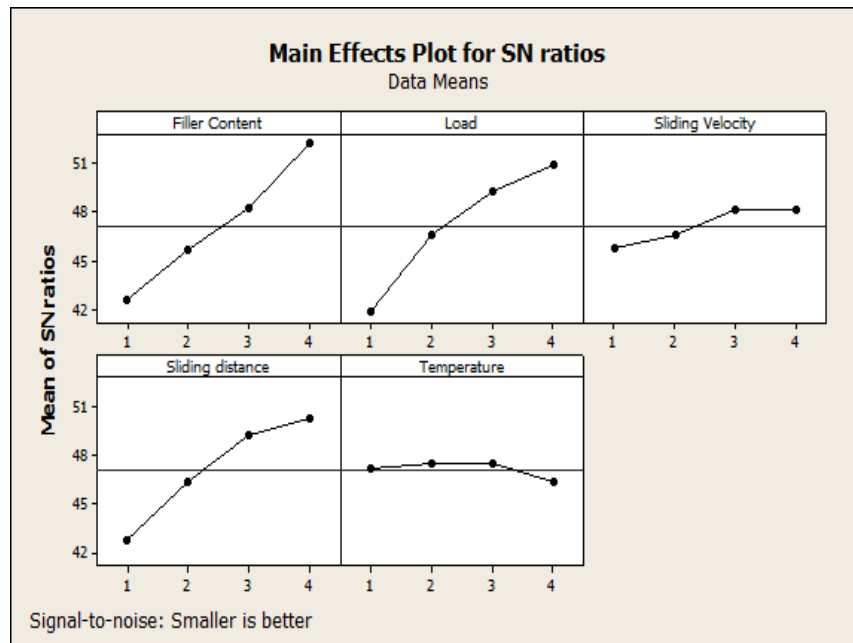
Fig 5.11 Effect of control factors on wear rate (Second set of composites)

5.4.3 Confirmation experiment

The confirmation experiment is the final test in the design of experiment process.The purpose of the confirmation experiment is to validate the results drawn from analysis. The confirmation experiment is performed by conducting a new set of factors $(A_3B_3C_3D_3E_2)$. The estimated S/N ratio for wear rate can be calculated with the help of following prediction equation:

$$\bar{\eta}_1 = \bar{T} + (\bar{A} - \bar{T}) + (\bar{B} - \bar{T}) + (\bar{C} - \bar{T}) + (\bar{D} - \bar{T}) \tag{5.5}$$

A new combination of factor levels A3, B3, C$_3$, D3 and E2 is used to predict wear rate through prediction equation and it is found to be η= 57.5895 db.

At the same level of parameters experimental test is conducted and the S/N ratio calculated for the same.

Table 5.4 Confirmation test S/N values.

	Predicted value	Experimental value
Level	$A_3B_3C_3D_3E_2$	$A_3B_3C_3D_3E_2$
S/N Ratio(db)	57.5895	56.78682

From this confirmation test we can conclude that this model is able to predict the results of wear rate up to a reasonable accuracy. An error of 1.3937% for the S/N ratio of wear rate is observed.

Chapter summary

1. Steady state wear rate for all the compositions is experimentally tested on different load, sliding velocity, sliding distance and temperature. Wear rate decreases with increase in the filler content which it was due to presence of ceramic particles and formation of mechanical mixed layer on wear surface.

2. Wear rate increases with increase in load, sliding velocity, temperature but the change in wear rate with the load was most significant.

3. SEM results show the surface morphology of the worn surface of composites in the different levels of factors. Wear Behavior on the fabricated composite can be easily observed from SEM images

4. From the Taguchi method it is concluded that the filler content and load are the most significant factors responsible for wear behavior of composites while temperature and sliding distance are least significant factors.

The next chapter presents the FEM analysis of the piston ring by using ANSYS software.

*****

In this chapter Finite element models are presented to analyze the stresses in a piston ring at different loading conditions like gas pressure, piston ring to cylinder contact and centrifugal forces. The induced stress and deformation are analyzed in these three loading conditions. The developed model given same properties of the fabricated composite 'C$_3$' for design based validation of the material

6.1 FINITE ELEMENT METHOD

Finite element method is a numerical analysis technique for obtaining approximate solutions to a wide variety of engineering problems. Although originally developed and applied to the broad field of continuum mechanics. Because of its diversity and flexibility as analysis tool, it is receiving much attention in engineering schools and industry. In more and more engineering situation today, it is necessary to obtain numerical solutions to problem rather than exact closed from solutions. The resourcefulness of the analyst usually comes to the rescue and provides several alternatives to overcome this dilemma. One possibility is to make simplifying assumption to ignore the difficulties and reduce the problem to one that can be handled sometimes this procedure works but more often than not it leads to series inaccurate or wrong answers.

Now that computers are widely available, a more viable alternative is to retain the complexities of the problem and to find an approximate numerical solution. A finite element model of a problem gives a piecewise approximation to the governing equations'. The basic premise of the finite element method is that a solution region can be analytically modeled or approximated by replacing it with an assemblage of discrete elements since these can be put together in a variety of ways, they can be put together in a variety of ways, and they can be used to represent exceedingly complex shape.

6.2 MODELING AND MESH GENERATION OF PISTON RING

Finite element analysis is a powerful tool, which can be used to study the behavior of any structural member subjected to any type of load. Even though the results are approximate, it predicts the chances of failure with more accuracy. Hence, in most of

the engineering analysis, it is mostly preferred. After calculating the dimensions, 3-d model of the piston ring is modeled in the ANSYS environment itself which is presented in fig. 6.1.

The piston ring model is developed in the ANSYS by using the proper dimensions as mention in Table 6.1. The developed model is given same properties of the fabricated composite 'C$_3$' for design based validation of the material.

Table 6.1 Dimensions of the piston ring model

	Outer dia(mm)	Internal dia(mm)	Thickness(mm)	Gap(mm)
Dimensions of ring	53	49	3	5
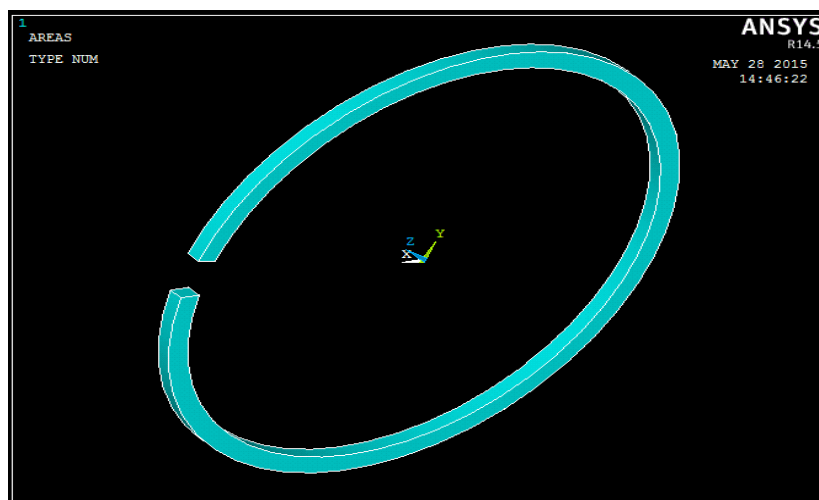
Figure 6.1 Piston ring

Element Type: SOLID185 is used for the three-dimensional modeling of solid structures. The element is defined by eight nodes having three degrees of freedom at each node: translations in the nodal x, y, and z directions. The element has plasticity, stress stiffening, large deflection, and large strain capabilities.
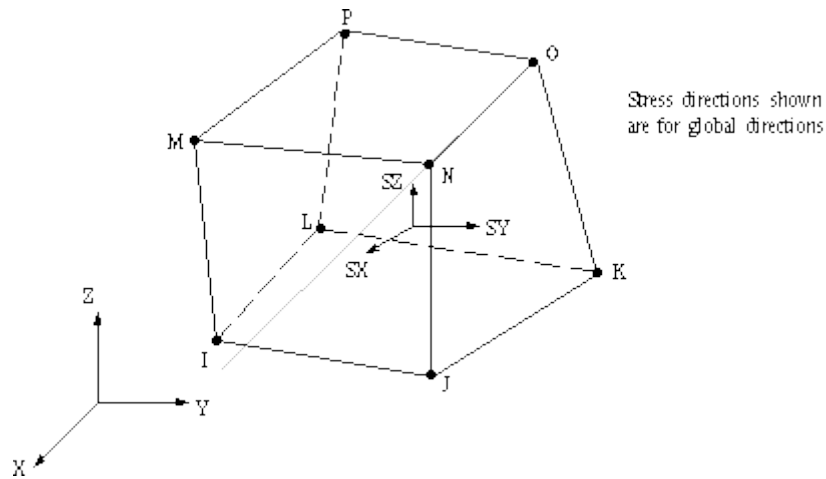
Figure 6.2 SOLID185 3-D Structural Solid [ANSYS Help]

Mesh Generation

The mesh size was determined using Mesh Control command. The piston ring is meshed by rough quad shaped free area mesh and each division of meshing is 2 mm as shown in fig. 6.3. After free mesh the mesh is refined at elements. The resulting final mesh consists of 21912 elements and 6157 number of nodes in total, have been taken to develop a piston ring for analysis.
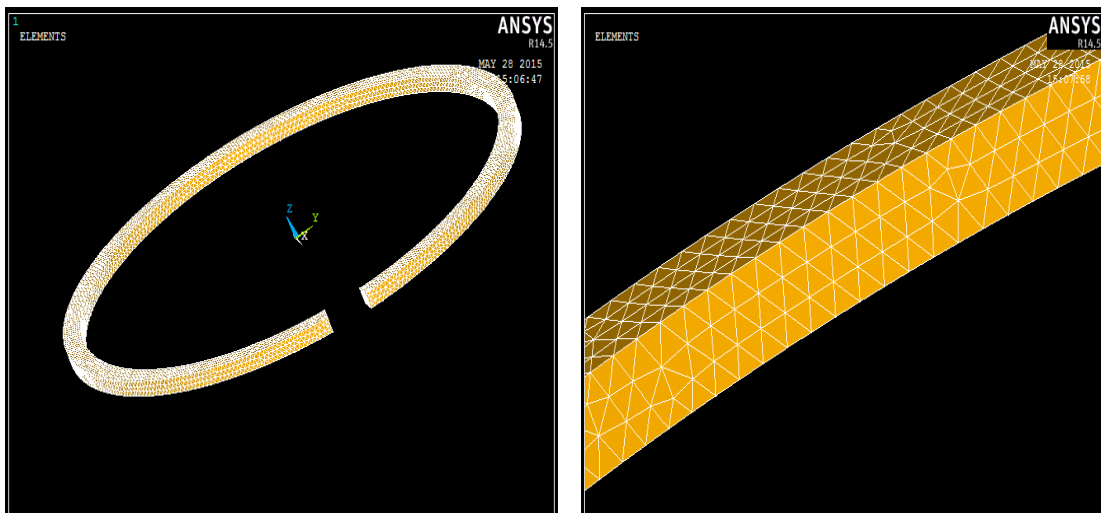
Figure 6.3 Meshing of ring

Material Properties:

Elastic modulus of 139 GPa and Poisson's ratio of 0.28 is taken for material.

Boundary condition and application of load

During analysis the following boundary conditions were considered as:-

1. Depending on dynamic condition of ring the boundary conditions are provided different for various critical conditions.

2. Depending on loading condition, the load is applied for simulation by using 'pressure on area' and 'force on nodes' command in the ANSYS software.

6.3 SIMULATION RESULTS OF PISTON RING

6.3.1 Expansion load on piston ring

Here the means of expansion is increase in diameter of the ring or increase in the size of gap. For this condition an internal pressure of 10 MPa is applied on the inner phase of the ring. In the actual condition inside the engine this expansion load is generated because of combustion gas pressure acting at the back of the ring. All the degree of freedom of the ring's one end (cross-section) are restricted. The von mises stress by the nodal solution is shown in fig.6.4. It can observed that the maximum stress is generated at the inner mid-section of the ring.
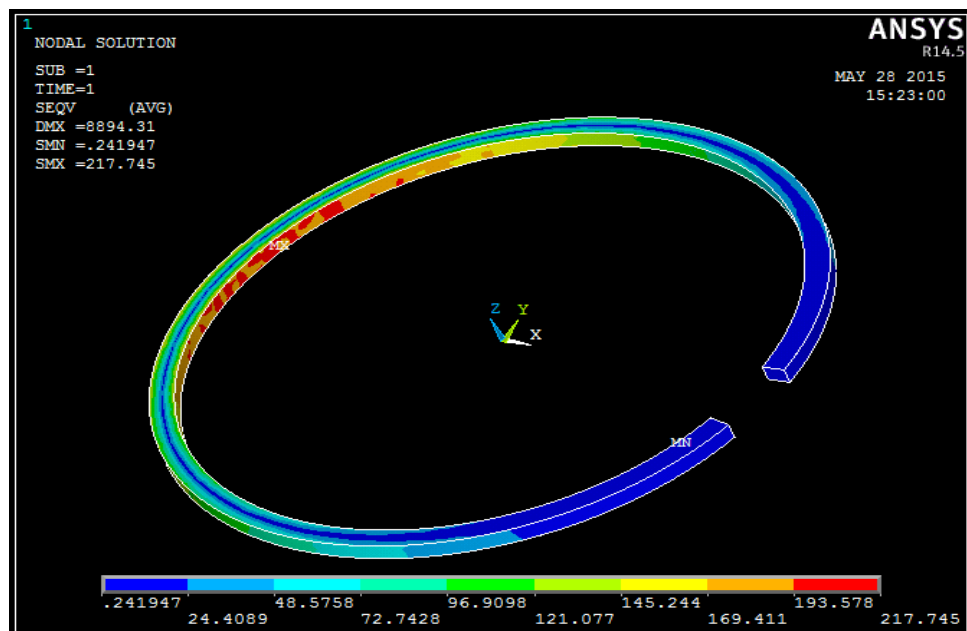
Figure 6.4 Stress developed in ring under expansion load

6.3.2 Compression load on piston ring

It is the condition in which stress is developed in ring due to contact load between cylinder and ring. Now in this condition load is applied at the outer area of the ring which generate the compression in ring means decrease in diameter of ring i.e. decrease in gap. The pressure of 15MPa is applied at the outer surface of the piston

ring. The one face area of the ring is fixed. Again the maximum stress is developed at the mid-section of the ring. Von mises stress solution is shown in fig.6.5.
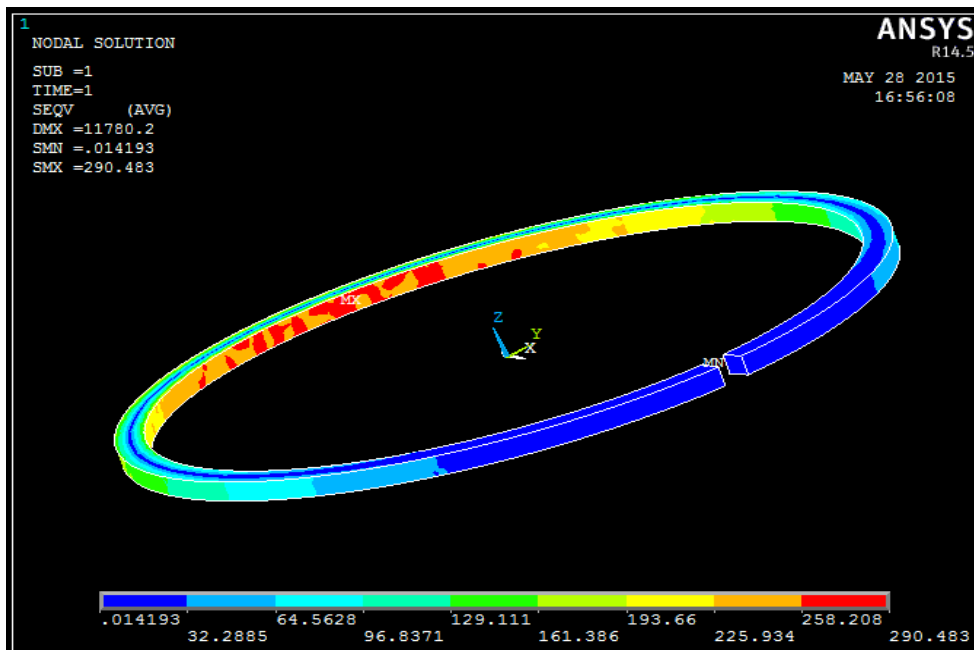
Figure 6.5 Stress developed in ring under compressive load

6.3.3 Bending load on piston ring

The bending of the ring is most critical in the design criteria. The main cause of failure of piston ring is this bending load only. This is developed due to secondary motion of the piston or non-uniform distribution of the gas pressure over the ring. So it can be divided into two parts:

(1)Point load: It is due to secondary motion of the ring in which there is more contact forces are generated at some points due to tilting of the piston ring which. In this condition tree point load of 10N are applied at three different nodes. The maximum von-mises stress is developed in the idle position at mid dia section of the ring (Fig.6.6)
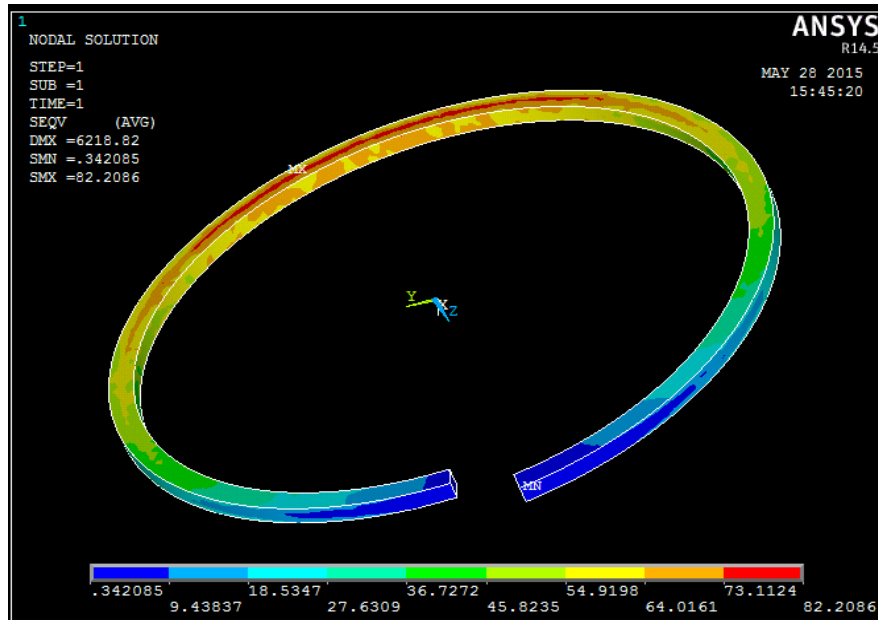
Figure 6.6 Stress developed in ring under point load

(2)Uniformly distributed load: this type of stress in the ring is generated due to the non-uniform distribution of gas pressure over the ring. For simulation of this loading condition pressure of 5 MPa is applied at upper surface of the ring. The von-mises stress nodal solution is shown in fig. 6.7

Figure 6.7 Stress developed in ring under uniformly distributed bending load

6.3.4 Combined loading condition:

Now finally to see the combined effect of different loads this simulation is performed.

Here the compression and bending of ring can be seen simultaneously. The von-mises

nodal solution is shown in Fig. 6.8.
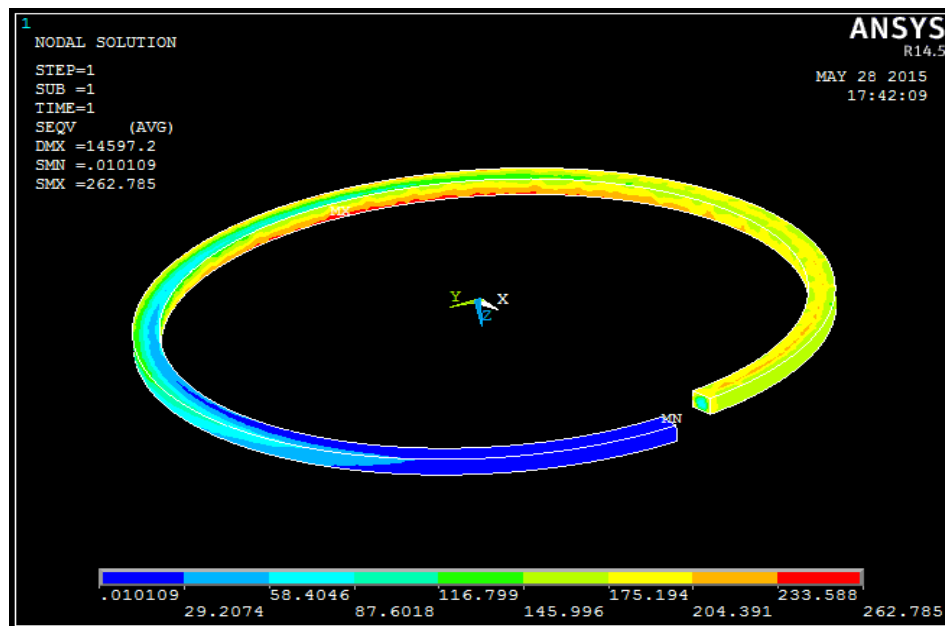
Figure 6.8 Stress developed in ring under combined loading condition

Chapter Summery

The successfully ASYS based simulation of the piston ring is done at varying
conditions of load. And the design based confirmation is given for newly fabricated
composite material for the piston ring.

**The next chapter presents the comparative analysis of conventionally used
material and the proposed material.**

*****

This Chapter presents a comparison between the existing material for piston ring and the proposed materials on different criteria related to piston ring performance. Here cast iron and steel are taken as the existing material for piston ring and which compared with fabricated materials C_3(Al7075+2%graphite+9%garnet) and $C'3$(Al7075+2%graphite+9%garnet). Rating is done from D to A^+, D for the very poor and A^+ for the excellent.

7.1 CATEGORY WISE COMPARATIVE ANALYSIS

7.1.1 Fuel Economy
Cast Iron = C   Coated steel = C^+ Composite C_3 = A   Composite C'_3 = A^+

Fuel economy or fuel consumption is the measurement of how much fuel the automobile's internal combustion engine uses over a given distance i.e kilometers run per unit liters of fuel. This category is important to validate the assessment of replacing cast iron ring by aluminum composite. Engine fuel economy will become more important to automakers in the near future as demand is continuously increasing while the supply resources are limited. Researching the alternatives has led to the conclusion that all by replacing the cast iron piston ring the with fabricated composites the fuel economy will surely improve because of reduction in weight, better conformity between piston ring and cylinder liner and reductionin frictional loses.

7.1.2 Engine Emissions
Cast Iron = C   Coated steel= C^+ Composite C_3 = A   Composite C'_3= A^+

Engine emissions are the byproducts of the automobile engines combustion processes that exit the tailpipe of an automobile and enter the atmosphere. The subject of automobile emissions has become more important in recent times due to the increased awareness of their impact to the planet's ecosystem. The results here for this comparison are the same as the fuel economy results. Each alternative holds a slight advantage over the previous solution. This stems from the fact that each alternative

slightly increases the fuel efficiency of the engine which will decrease the engine emissions by a small amount.

7.1.3 Life of piston ring
Cast Iron = C   Coated steel= B   Composite $C_3 = A^+$ Composite $C'_3 = A$

The life of any component is most important thing to be considered. If the piston ring fails to perform its intended function, it creates severe problems like seizing of piston-cylinder system. Composites of garnet/graphite or flyash/graphite filled aluminium have longer life as compared to the cast iron and coated steel. It was due to the more wear resistance,better mechanical and thermal properties of the composite.

7.1.4 Previous Application as piston ring material
Cast Iron =A   Steel = B^+ Composite C_3=D   Composite C'_3=D

It gives confidence to the present work to see the number of alternative materials and coatings used and a continuous new adaption of material and coatings can be seen for piston ring it shows that the automobile industries are searching for a better material to be used as piston ring material. In the recent development for more fuel economic engines automobile industries replaced different part with aluminium like piston, cylinder block etc. A series of material can be listed for the piston ring starting from cast iron which is most used material for the piston ring and then steel, ductile iron etc. Different coating like molybdenum disulfide coating, ceramic coating, PTFE coating are to improve the performance at some extent. All these are done by the researchers but very few of them tried composite for the piston ring which can perform the required role very efficiently.

7.1.5 Friction between cylinder block and piston rings
Cast Iron = C   Coated steel= C^+ Composite $C_3 = B^+$ Composite C'_3=A

The friction between the cylinder block bore material and the piston rings is the single biggest contributor to the loss of power in an internal combustion engine. Limiting this friction goes a long way in increasing the fuel efficiency of an automobile outside of reducing vehicle weight.   The best alternative for reducing friction is the 9%flyash/2%graphite reinforced aluminium composite. The presence of graphite and flyash reduces the surface friction due to the lubricating effect. The more evenly the particles are dispersed in the aluminum, the better the material can provide a smooth

sliding surface while maintaining the ability to retain oil for lubricating purposes. Cast iron is the basis of the comparison and demonstrates acceptable performance.

7.1.6 Wear Resistance
Cast Iron = B   Coated Steel=B$^+$ Composite C$_3$=A$^+$ Composite C'$_3$=A

Resistance to wear from a sliding surface is one of the key characteristics that a piston ring material needs to exhibit. The harsh environment of an internal combustion engine can easily damage softer materials. Several researchers have performed extensive wear resistance testing of the alternatives for cast iron for piston ring material. The results show that wear resistance of the composite are excellent which was due to the presence of the garnet, graphite and flyash particles. The fiber reinforced composites and hypereutectic Al-Si don't rate as highly compared to the alternatives because their wear resistance is based on the dispersed particles of the additive elements that give the alternative materials sufficient wear resistance. If the dispersed particles are large enough and evenly mixed, wear can occur where large areas of the softer parent aluminum material is prevalent.

7.1.7 Scuffing Resistance
Cast Iron = A   Coated Steel=B$^+$ Composite C$_3$= B+   Composite C'$_3$=B

A material's ability to resist scuffing is another important characteristic. As discussed earlier, scuffing occurs right after the engine is turned on and the cylinder block and piston ring are still cold. The importance of scuffing has led several researchers to develop scuffing resistance testing comparing the alternative materials to cast iron for cylinder block bore surfaces. The scuffing resistance testing had similar results as the wear resistance testing, which would be expected because both tests have similar setups and rely on similar material behavior. Simply stated, the test involves a reciprocating load that is cycled over the test material to examine the action of the piston and piston rings on the cylinder bore surface. Material/scuffing is observed and recorded. Cast iron again demonstrated the best scuffing resistance followed by the 9%Garnet/Graphite filled aluminium composite (C3).

7.1.8 Thermal Conductivity
Cast Iron = C   Coated Steel=C$^+$ Composite C$_3$ = A   Composite C'$_3$ =B$^+$

Thermal conductivity is the property of a material's ability to conduct heat. The thermal conductivity of the piston ring material is important in controlling the operating temperature of the internal combustion engine. The piston rings ability to gain or lose heat impacts the efficiency of the combustion process which in turn impacts the engines fuel efficiency and emissions. The more thermally conductive the piston ring material is, the easier it is for the cooling system to maintain a constant temperature through the engine assembly. This eliminates the possibility of hot spots in the piston ring which over time can lead to cracking and failure of the ring. Aluminum is three times more thermally conductive than cast iron.

7.1.9 Production Costs
Cast Iron = A   Coated Steel=B   Composite C$_3$ = C   Composite C'$_3$ = C

The material's production costs are those associated with the material procurement, casting process, specialized tooling, coating process (where applicable) and post-cast machining. As for the manufacturing cost associated with product, the cast iron piston rings are the cheapest solution. It is difficult to cast composites, special arrangements are required for proper fabrication of the composites.

7.1.10 Mass Production Feasibility
Cast Iron = A   Coated Steel=B   Composite C$_3$ = C   Composite C'$_3$= C

The alternative choices to using cast iron liners for aluminum cylinder blocks may be feasible on a mass production scale. It's an important parameter in this comparison. Currently cast iron piston rings are used in the majority of the production of vehicles. Assuming that in the future the automakers need to move away from cast iron liners because of the increased fuel economy standard, composites mass production can be adapted by acquiring the required set for the composite fabrication. The initial cost must be high but in long term it will be feasible to adapt this process.

The next chapter presents the summary and conclusion of the present research work.

*****

8.1 INTRODUCTION

The research reported in this thesis broadly consists of:

➢ Study of mechanical and tribological behavior of two different sets of composite first is garnet/graphite filled and second is flyash/graphite filled.

➢ Comparison of experimental and FEM modeling based results

➢ Design and performance based validation of fabricated composite for piston ring material.

8.2 CONCLUSIONS

This simulation and experimental investigation on particulate filled 7075 alloy hybrid composites has led to the following specific conclusions:

1. The void content of the fabricated composites increases with increased filler content. The void content of Al7075 alloy composites increases from 0.726 % to 1.210% and 0.726 % to 1.551% with the increased garnet and flyash wt.-% from 0 % to 9 % respectively. The hardness of the parent matrix also increases with the addition of ceramic particles.

2. The tensile strength of Al7075 alloy composites is found to be higher than the unfilled alloy composites for both experimental and FEM results. The maximum percentage error for tensile strength calculated experimentally and by FEM is found to be 6.24 % and 7.54 for garnet/graphite and flyash/graphite filled Al7075 alloy composite, which is within the acceptable range. The impact energy of the garnet/graphite and flyash/graphite filled Al7075 alloy composites decreases with the increased garnet and flyash content.

3. Steady state reciprocating wear rate (mm^3/m) for all the compositions is determined for different load, sliding velocity, sliding distance and temperature. The wear rate increases with increase in load, sliding velocity and temperature while the increase in wear rate with respect to load is more significant. The improved wear resistance behavior is observed for the fabricated composites as compare to the parent alloy.

4. The wear samples observed under SEM observation shows formation of oxide layers i.e. mechanical mixed layer of iron and aluminium oxides, which is

responsible for the improved wear resistance of the composites. The sliding wear pattern and the cracks are also clearly observed from the SEM results.

5. Taguchi Method is used for the optimization of different wear parameters involved in the experiment. And it is found that the load is the most significant parameters followed by reinforcement and sliding velocity. Temperature and sliding distance are least significant parameters

6. FEM analysis of the ring shows the design validation of the proposed material for the piston ring. And it observed that the stresses developed in the piston design with the fabricated material are under acceptable limits.

7. In the comparative analysis, the comparison of the conventionally used material and the fabricated composite are shown based on different criteria essential for a material to be used as piston rind. And it was observed that the with some improvement the proposed material can be used as piston ring material

8.3 SCOPE FOR FUTURE WORK

With regard to suggestions for the future work, the following points are deemed to merit further investigation:

1. Other available filler can also be used and the proper study for that should be done.

2. In place of stir-casting other method for fabrication of composite as powdwer metallurgy can be adopted.

3. Experimental set-up can be improved to see the more actual results for the ring performance.

4. Actual ring of the fabricated composite can be fabricated for real condition analysis of the material.

<div align="center">*****</div>

REFERENCES

[1] Open government data platform India. [Online]https://data.gov.in.

[2] THE AIR (PREVENTION AND CONTROL OF POLLUTION) ACT, 1981, Delhi, DEPARTMENT OF ENVIRONMENT , 1983.

[3] Yeow-Chong Tan, Zaidi Mohd Ripin,(2011),Frictional behavior of piston rings of small utility two-stroke engine under secondary motion of piston, Tribology International 44,592–602

[4] John J. Truhana,Jun Qu, Peter J. Blau,(2005), A rig test to measure friction and wear of heavy duty diesel engine piston rings and cylinder liners using realistic lubricants.

[5] O.P. Singh,Yogesh Umbarkar,T. Sreenivasulu,E. Vetrivendan,M. Kannan, Y.R. Babu, (2013), Piston seizure investigation: Experiments, modeling and future challenges, Engineering Failure Analysis,28,302–310

[6] E. Ramjee and K. Vijaya Kumar Reddy, "Performance analysis of a 4-stroke SI engine using CNG as an alternative fuel", Indian Journal of Science and Technology, Vol. 4, No. 7, July 2011.

[7] Peter Andersson, Jaana Tamminen & Carl-Erik Sandström,(2002), Piston ring tribology,A literature survey, VTT Industrial Systems, VTT research notes 2178.

[8] Jayakumar Lakshmipathy,Balamurugan Kulendran (2014),Reciprocating wear behavior of 7075Al/SiC in comparison with6061Al/Al2O3 composites.

[9] Maass, H. and Klier, H. Kräfte, Forces, moments and their equilisation in internal combustion engines / in German. Die Verbrennungskraftmaschine, Neue Folge, Band 2. Vienna, Austria, 1981, Springer-Verlag, 422 p. ISBN 3-211-81677-1.

[10] Ejakov, M. A., Diaz, A. R. and Chock, H. J. Numerical optimization of ring-pack behavior. Society of Automotive Engineers, Inc., 1999, SAE Paper 1999-01-1521, 12 p.

[11] Dowson, D. Piston assemblies; background and lubrication analysis. In: Taylor, C.M. (ed.). Engine Tribology. Elsevier, 1993, Tribology series, 26, pp. 213–240. ISBN 0-444-89755-0

[12] Röhrle, M. D. Pistons for internal combustion engines − fundamentals of piston technology, MAHLE GmbH. Verlag Moderne Industrie. Landsberg/Lech, Germany.1995. p. 70

[13] Haddad. S. D. and Tjan, K.-T. An analytical study of offset piston and crankshaft designs and the effect of oil film on piston slap excitation in a diesel engine. Mechanism and Machine Theory, 30(1995)2, pp. 271−284.

[14] Chittenden R. J. and Priest M. Analysis of the piston assembly, bore distortion and future developments. In: Taylor, C.M. (ed.). Engine Tribology. Elsevier, 1993, Tribology series, 26, pp. 241−270. ISBN 0-444-89755-0.

[15] Dufrane, K. F. Wear performance of ceramics in ring/cylinder applications. Journal of the American ceramic Society, 72(1989)4, pp. 691−695.

[16] Haselkorn, M. H. and Kelley, F. A. Development of wear resistant ceramic coatings for diesel engines, SAE Proceedings of the Annual Automotive Technology Development Contractors Co-ordination Meeting, 1992, pp. 417−424.

[17] Glidewell, J. and Korcek, S. Piston ring / cylinder bore friction under flooded and starved lubrication using fresh and aged engine oils. Society of Automotive Engineers,Inc., 2010, SAE Paper 982659, 10 p.

[18] Glaeser, W. A. and Gaydos, P. A. Development of a wear test for adiabatic diesel ring and liner materials. ASTM 2009, Proc Symp wear test selection for design and application, Dec 2 1992. Miami, FL, USA, ASTM Philadelphia PA, 0066-0558 ASTTA8, ASBN 0-8031-1856-2, pp. 1−16.

[19] Dearlove, J. and Cheng, W. K. Simultaneous piston ring friction and oil film thickness measurements in a reciprocating test rig. In: Recent snapshots and insights into lubricant tribology (SAE SP-1116), Warrendale, USA, 2012, SAE International, SAE Technical Paper Series 952470, pp. 29−39.

[20] Takiguchi, M., Ando, H., Takimoto, T. and Uratsuka, A. Characteristics of friction and lubrication of two-ring piston. JSAE Review, 17(2011)1, pp. 11−16.

[21] Nitesh Mittal, Robert Leslie Athony, Ravi Bansal, C. Ramesh Kumar, (2013),Study of performance and emission characteristics of a partially coated LHR SI engine blended with n-butanol and gasoline, Alexandria Engineering Journal,52, 285−293

[22] S.V. Kamat, S.P. Hirth and R.M. Mehrabin, 1989, Mechanical properties of particulate-reinforced aluminum-matrix composites, Acta Metallurgy, 37, 2395.

[23] Breval E, (1995). Synthesis routes to metal matrix composites with specific properties: a review, Composites Engineering, Vol. 5, No. 9. pp. 1127-l133.

[24] Mahendra, K.V. and Radhakrishna, K., 2007, "Castable Composites and their Application in Automobiles", Proceedings of the Institution of Mechanical Engineers, Part D: Journal of Automobile Engineering, 221, pp. 135-140.

[25] Rohatgi, P.K., Asthana, R. and Das, S., 1986, Solidification, Structures, and Properties of Cast Metal-Ceramic Particle Composites, International Metals Reviews, 31, pp. 115-139.

[26] Lakshmi S, Lu L, Gupta M, 1998, In situ preparation of TiB2 reinforced Al based composites. J Mater Process Technol;73:160–6.

[27] Natarajan S, Naraynasamy R, Kumaresh Babu SP, Dinesh G, Anil kumar B, Sivaprasad K., 2009, Sliding wear behaviour of Al 6063/TiB2 in situ composites at elevated temperatures. Mater Des,30:2521–31.

[28] B.N. Pramila Bai, B.S. Ramasesh, M.K. Surappa. 1992, Dry sliding wear of A356–Al–SiCp composites. Wear 157:295–304.

[29] S.C. Sharma, 2001, The sliding wear behavior of Al6061–garnet particulate composites, Wear, 249, 1036–1045

[30] P.R.S. Kumar, S. Kumarn, T. Srinivasa Rao, S. Natarajan, 2010, High temperature sliding wear behavior of press-extruded AA6061/fly ash Composite, Materials Science and Engineering A 527, 1501–1509

[31] Jayakumar Lakshmipathy, Balamurugan Kulendran, 2014, Reciprocating wear behavior of 7075Al/SiC in comparison with 6061Al/Al2O3 composites, Int. Journal of Refractory Metals and Hard Materials 46 (2014) 137–144.

[32] Himanshu Kala, K.K.S Mer, Sandeep Kumar, 2014, A Review on Mechanical and Tribological Behaviors of Stir Cast Aluminum Matrix Composites, Procedia Materials Science 6, 1951 – 1960.

[33] S. Suresh, N. Shenbaga Vinayaga Moorthi, S.C. Vettivel, N. Selvakumar, 2014,Mechanical behavior and wear prediction of stir cast Al–TiB2 composites using response surface methodology, Materials and Design ,59 383–396

[34] J.F. Archard, Contact and rubbing of flat surfaces, J. Appl. Phys. 24,(1953) 981–988.

[35] S. Kumar, M. Chakraborty, V. Subramanya Sarma, B.S. Murty, 2008, Tensile and wear behaviour of in situ Al–7Si/TiB2 particulate composites, Wear 265, 134–142.

[36] Dipti Kanta Das, Purna Chandra Mishra, Saranjit Singh,Ratish Kumar Thakur,2014, Properties of ceramic-reinforced aluminium matrix composites - a review, J Mechanical and Materials Engineering,1:12.

[37] Adel Mahamood Hassan, Abdalla Alrashdan, Mohammed T.Hayajneh, Ahmad Turki Mayyas, 2009, Wear behavior of Al–Mg–Cu–based composites containing SiC particles, Tribology International 42, 1230–1238.

[38] Devaraju Aruria, Kumar Adepua, Kumaraswamy Adepub, Kotiveerachari Bazavadaa, Wear and mechanical properties of 6061-T6 aluminum alloysurface hybrid composites [(SiC + Gr) and (SiC + Al2O3)]fabricated by friction stir processing.

[39] K. Umanath, K. Palanikumar, S.T. Selvamani , 2013, Analysis of dry sliding wear behaviour of Al6061/SiC/Al2O3 hybrid metal matrix composites, Composites: Part B 53,159–168

[40] A.N. Abdel-Azim, Y. Shash, S.F. Mostafa, A. Younan, 1995, Casting of 2024-A1 alloy reinforced with A12O3 particles, Journal of Materials Processing Technology 55, 199-205.

[41] Llorca J and Gonzalez C, (1998). Microstructural factors controlling the strength and ductility of particle-reinforced metal-matrix composites, J. Mech. Phys. Solids, Vol. 46. No. 1, pp. 1-28.

[42] K.L. Tee, L. Lu, M.O. Lai, 1999, Synthesis of in situ Al-TiB2 composites using stir cast route, Composite Structures 47, 589-593.

[43] Tjong S.C and Ma Z.Y, (2000). Microstructural and mechanical characteristics of in situ metal matrix composites, Materials Science and Engineering, 29:49-113.

[44] Veeresh Kumar, GB, Rao, CSP, Selvaraj, N, & Bhagyashekar, MS. (2010). Studies on Al 6061-SiC and Al 7075-Al2O3 metal matrix composites. Journal of Minerals & Materials Characterization & Engineering, 9(1), 43–55. USA.

[45] Ju D.Y, (2000). Simulation of thermo-mechanical behavior and interfacial stress of metal matrix composite under thermal shock process, Composite Structures, 48:113-118.

[46] Ruggles M.B, (1997). Experimental investigation of uniaxial and biaxial rate-dependent behavior of a discontinuous metal-matrix composite at 538 °C. Composites Science and Technology, 51:307-318.

[47] Spiridonova I. and Sukhova O, (2002). Cr-20Ti-10C particulate metal matrix composites, physics and chemistry of solid state, v. 3, No.3, p. 503-507.

[48] Taha M.A and El-Mahallawy N.A.E, (1999). Metal–matrix composites fabricated by pressure-assisted infiltration of loose ceramic powder, Journal of Materials Processing Technology, 73:139–146.

[49] Cordovilla C.G, Narciso J and Louis E, (1996). Abrasive wear resistance of aluminium alloy /ceramic particulate composites, Wear, 192:170-177.

[50] K.K. Alaneme, B.O. Ademilua, M.O. Bodunrin, 2013, Mechanical Properties and Corrosion Behaviour of Aluminium Hybrid Composites.

[51] Kouzeli M, Weber L, Marchi C.S and Mortensen A, (2001). Influence of damage on the tensile behavior of pure aluminium reinforced with $\geq$ 40 vol. pct alumina particles, Actamater, 49:3699–3709.

[52] X.M. Li, M.J. Stranik, Effect of compositional variations on characteristics of coarse intermetallic particles in overaged 7000 aluminium alloys, Mater. Sci. Technol. 17 (2001) 1324–1328.

[53] A.N. Abdel-Azim, M.A. Kassem, Z.M. El-Baradie, M. Waly, 2002, Structure and properties of short alumina fibre reinforced AlSi18CuNi produced by stir casting, Materials Letters 56, 963– 969.

[54] Tzamtzis S, Barekar N.S, Babu N.H, Patel J, Dhindaw B.K and Fan Z, (2009). Processing of advanced Al/SiC particulate metal matrix composites under intensive shearing – A novel Rheo-process, Composites: Part A, 40:144–151.

[55] Xu N and Zong B.Y, (2008). Stress in particulate reinforcements and overall stress response on aluminium alloy matrix composites during straining by analytical and numerical modeling, Computational Material Science, 43:1094-1100.

[56] Zong B.Y, Zhang F, Wang G and Zuo L, (2007). Strengthening mechanism of load sharing of particulate reinforcements in a metal matrix composite, J Mater Sci, 42:4215–4226.

[57] Chou S.N, Huang J.L, Lii D.F and Lu H.H, (2007). The mechanical properties and microstructure of Al_2O_3/aluminum alloy composites fabricated by squeeze casting, Journal of Alloys and Compounds, 436:124–130.

[58] M. Kok, 2006, Abrasive wear of Al2O3 particle reinforced 2024 aluminium alloy composites fabricated by vortex method, Composites: Part A 37,457–464.

[59] Keneth Kanayo Alaneme, Idris B. Akintunde, Peter Apata Olubambib, Tolulope M. Adewale, 2013, Fabrication characteristics and mechanical behavior of rice husk ash–Alumina reinforced Al-Mg-Si alloy matrix hybrid composites, J. Mater. Res. Technol. 2(1):60-67.

[60] Mahendra Boopathi, K.P. Arulshri , N. Iyandurai, 2013, Evaluation of mechanical properties of aluminium alloy 2024 reinforced with silicon carbide and fly ash hybrid metal matrix composites, American Journal of Applied Sciences, 10 (3): 219-229.

[61] Jayaram, V, & Biswas, SK. (1999). Wear of Al2O3-SiC-(AlSi) melt oxidised ceramic composites. Wear, 225–229, 1322–1326. Elsevier, United Kingdom.

[62] Kumar G.B.V, Rao C.S.P and Selvaraj N, (2011). Mechanical and tribological behavior of particulate reinforced aluminum metal matrix composites – a review, Journal of Minerals & Materials Characterization & Engineering, Vol. 10, No.1, pp.59-91.

[63] ,S.C. Sharma, G. Ranganath ,Dry sliding wear of garnet reinforced zinc/aluminum metal matrix composites. Wear 2001;251:1408–1413.

[64] S.C. Sharma,(2001),The sliding wear behavior of Al6061–garnet particulate composites, Wear,249,1036–1045

[65] Sannino, A.P. and Rack, H.J. 1995. Dry Sliding Wear of Discontinuously Reinforced

[66] Narayan M, Surappa M.K and Bai B.N.P, (1995). Dry sliding wear of Al alloy 2024-A1$_2$0$_3$ particle metal matrix composites, Wear, 181-183:563-570.

[67] Pruthviraj R. D., (2011). Wear characteristics of chilled zinc-aluminium alloy reinforced with silicon carbide particulate composites, Res. J. Chem. Sci., Vol. 1 (2):17-24.

[68] Wang S.R, Geng H.R, Wang Y.Z and Zhang J.C, (2006). Microstructure and fracture characteristic of Mg–Al–Zn–Si$_3$N$_4$ composites, Theoretical and Applied Fracture Mechanics, 46:57–69.

[69] Ye H, (2003). An overview of the development of Al-Si-alloy based material for engine applications, Journal of Materials Engineering and Performance, 12:288-297.

[70] Prasad S.V and Asthana R, (2004). Aluminum metal–matrix composites for automotive applications: tribological considerations, Tribology Letters, Vol.17, No.3:445-453.

[71] Arik H, Ozcatalbas Y and Turker M, (2006). Dry sliding wear behavior of in situ Al–Al$_4$C$_3$ metal matrix composite produced by mechanical alloying technique, Materials and Design, 27:99–804.

[72] Kennedy F.E, Balbahadur A.C and Lashmore D.S, (1997). The friction and wear of Cu-based silicon carbide particulate metal matrix composites for brake applications, Wear, 203-204:715-721.

[73] Lim L.G and Dunne F.P.E, (1996). The effect of volume fraction of reinforcement on the elastic-viscoplastic response of metal-matrix composites, Int. J. Mech. Sci. Vol. 38, No. l, pp. 19- 39.

[74] Dogan O.N, Hawk J.A, Tylczak J.H, Wilson R.D and Govier R.D, (1999). Wear of titanium carbide reinforced metal matrix composites, Wear, 225–229:758–769.

[75] Gurcan A.B and Baker T.N, (1995). Wear behaviour of AA6061 aluminium alloy and its composites, Wear, 188:185-191.

[76] C. G. Cordovilla, J. Narciso, E, Louis. Abrasive wear resistance of aluminum alloy /ceramic particulate Composites. Wear 1996;192:170-177.

[77] Zarghani A.S, Bozorg S.F.K and Hanzaki A.Z, (2011). Wear assessment of Al/Al$_2$O$_3$ nano-composite surface layer produced using friction stir processing, Wear, 270: 403–412.

[78] Shivamurthya R.C and Surappa M.K, (2011). Tribological characteristics of A356 Al alloy–SiC$_P$ composite discs, Wear, 271:1946– 1950.

[79] P. S. Shenoy and A. Fatemi, " Dynamic Analysis of Loads and Stresses in Connecting Rods", Journal of Mechanical Engineering Science, 2006, Vol. 220, No. 5.

[80] P. S. Shenoy and A. Fatemi, " Connecting Rod Optimization for Weight and Cost Reduction", SAE Paper No. 2005-01-0987, SAE 2005 Transactions: Journal of Materials and Manufacturing .

[81] P. Gudimetal P. and C. V. Gopinath, " Finite Element Analysis of Reverse Engineered Internal Combustion Engine Piston",© King Mongkut's University of Technology,Bangkok, Thailand, AIJSTPME, 2009.

[82] Ajay Raj Singh, Dr. Pushpendra Kumar Sharma,(*2014*) Design, Analysis and Optimization of Three Aluminium Piston Alloys Using FEA, Journal of

Engineering Research and Applications,ISSN : 2248-9622, Vol. 4, Issue 1 Version 3, pp.94-102

[83] Segurado J and LLorca J, (2004). A new three-dimensional interface finite element to simulate fracture in composites, International Journal of Solids and Structures, 41:2977–2993.

[84] Prabua S.B, Karunamoorthy L and Kandasami G.S, (2004). A finite element analysis study of micromechanical interfacial characteristics of metal matrix composites, Journal of Materials Processing Technology, 153–154:992–997.

[85] Ganguly P and Poole W.J, (2003). In situ measurement of reinforcement stress in an aluminum-alumina metal matrix composite under compressive loading.

[86] Prabu S.B and Karunamoorthy L, (2008). Microstructure-based finite element analysis of failure prediction in particle-reinforced metal–matrix composite, Journal of Materials Processing technology, 207:53–62.

[87] Ying Yu, Hitoshi Ishii, Keiichiro Tohgo, Young Tae Cho, Dongfeng Diao, 1997. Temperature dependence of sliding wear behavior in SiC whisker or SiC particulate reinforced 6061 aluminum alloy composite. Wear, 213, 21-28.

[88] How, H.C, Baker, T.N., 1997. Dry sliding wear behaviour of Saffil-reinforced AA6061 composites. Wear. 210, 263-272.

[89] Hongya Xua, Fen Wangb, Jianfeng Zhub, Yuxing, Xie, 2011. Microstructure and Mechanical Properties of HoAl-Al2O3/Ti Al Composite, Materials and Manufacturing Processes, 26 (4), 559 561.

[90] Taguchi G and Konishi S, (1987).Taguchi Methods: Orthogonal Arrays and Linear Graphs; Tools for Quality Engineering, American Supplier Institute Inc., Dearborn, MI.

[91] Taguchi G, (1990). Introduction to Quality Engineering, Asian Productivity Organization, Tokyo.

[92] Phadke M.S, (1989). Quality Engineering using Robost Design, Prentice- Hall, Materials and Design. vol. 31, pp. 837–849.

[93] Wu Y and Moore W.H, (1986). Quality Engineering: Product & Process Design Optimization, American Supplier Institute Inc., Dearborn, MI.

[94] Shoemaker A.C and Kackar R.N, (1988). A methodology for planning experiments in robust product and process design, Qual. Reliab. Eng. Int. 4:95–103.

[95] Phadke M.S and Dehnad K, (1988). Optimization of product and process design for quality and cost. Qual. Reliab. Eng. Int. 4:105–112.

[96] Surajit Sengupta. Wate absoption of jute needle-punched nonwoven fabric. Indian Journal of Fiber and Textile Research. 2009. vol. 34, pp. 345-351.

[97] B.N. Ramesh, B. Suresha. Optimization of tribological parameters in abrasive wear mode of carbon-epoxy hybrid composites. 2014. vol. 59, pp. 38-49.

[98] Siddhartha, Amar Patnaik, Amba D. Bhatt. Mechanical and dry sliding wear characterization of epoxy–TiO2 particulate filled functionally graded composites materials using Taguchi design of experiment. 2011. Materials and Design. vol.32, pp.615–627

[99] Amar Patnaik, Md Abdulla, Alok Satapathy, Sandhyarani Biswas, Bhabani K. Satapathy. A study on a possible correlation between thermal conductivity and wear resistance of particulate filled polymer composites. 2010. Materials and Design. vol. 31, pp. 837–849.

[100] PatnaikA, SatapathyA, MahapatraSS, DashRR.,2009,Tribo-performanceofpolyester hybrid composites: damage assessment and parameter optimization using Taguchi design. Mater Des;30:57–67.

[101] Srimant Kumar Mishra, Sandhyarani Biswas, Alok Satapathy,2014, A study on processing, characterization and erosion wear behavior of silicon carbide particle filled ZA-27 metal matrix composites, Materials and Design 55, 958–965

[102] Siddhartha Prabhakar N, Radhika.N , Raghu.R ,2014, Analysis of tribological behavior of aluminium/B4C composite under dry sliding motion, Procedia Engineering 97 ,994 – 1003

[103] A.Baradeswaran, A.Elayaperumal, R. Franklin Issac,2013, A Statistical Analysis of Optimization of Wear Behaviour of AlAl2O3 Composites Using Taguchi Technique, Procedia Engineering, 64, 973 – 982

[104] S. Basavarajappa, G. Chandramohan , J. Paulo Davim,2007, Application of Taguchi techniques to study dry sliding wear behaviour of metal matrix composites, Materials and Design 28 , 1393–1398

[105] Y. Sahin, 2005, Optimization of testing parameters on the wear behaviour of metal matrix composites based on the Taguchi method, Materials Science and Engineering A 408, 1–8

[106] Ravindra Singh Rana, Rajesh Purohib, Anil kumar Sharma, Saraswati Rana,2014, Optimization of Wear Performance of Aa 5083/10 Wt. % Sicp Composites Using Taguchi Method Procedia Materials Science 6, 503 – 511

[107] S. Rajesh, A. Gopala Krishna, P. Rama Murty Raju, M. Duraiselvam, 2014, Statistical Analysis of Dry Sliding Wear Behavior of Graphite Reinforced Aluminum MMCs, Procedia Materials Science 6 ,1110 – 1120

[108] S.S. Mahapatraa,*, Amar Patnaikb,2009, Study onmechanical anderosion wear behavior ofhybrid composites using Taguchi experimental design, Materials and Design 30 ,2791–2801

[109] T.S. Kiran M. Prasanna Kumar b, S. Basavarajappa c, B.M. Viswanatha, (2014) Dry sliding wear behavior of heat treated hybrid metal matrix composite using Taguchi techniques, Materials and Design 63, 294–304

*****

- **Shivam Mishra**, Abhisek Pandey, Amar Patnaik, 2015, Optimization of Reciprocating Wear Performance of Garnet & Graphite reinforced Al7075 alloy hybrid Composite Using Taguchi Method, National Conference on Futuristic Approaches in Civil & Mechanical Engg, Maharshi Arvind Inst of Engg and Tech.,Jaipur, 24th & 25th march.

- **Shivam Mishra**, Vinod Kumar Gautam, Amar Patnaik, 2015, Study of Motion, Forces, friction and wear with effect of lubrication in Piston Ring, National Conference on Futuristic Approaches in Civil & Mechanical Engg, Maharshi Arvind Inst of Engg and Tech.,Jaipur, march 24th -25th.

- Abhisek Pandey, **Shivam Mishra**, Amar Patnaik, 2015, Review on graphite reinforced Metal Matrix Composite, National Conference on Futuristic Approaches in Civil & Mechanical Engg, Maharshi Arvind Inst of Engg and Tech.,Jaipur, 24th & 25th march.

- **Shivam Mishra**, Abhisek Pandey, Amar Patnaik, 2015, Analysis of Tribological behavior of Fly-ash & Graphite reinforced Al7075 alloy under reciprocating motion, International conference on Emerging & Futuristic Trend in Engg and Technology, Maharaja Agrasen Inst of Tech,Solan, HP, May 8th-9th.

- Abhisek Pandey, **Shivam Mishra**, Amar Patnaik, 2015, A Review on Failure of Ball Bearing under Various Loading Conditions, International conference on Emerging & Futuristic Trend in Engg and Technology, Maharaja Agrasen Inst of Tech,Solan, HP, May 8th-9th.